



UNIVERSITÀ  
DEGLI STUDI  
DI PADOVA

Sede Amministrativa: Università degli Studi di Padova

Dipartimento della Salute della Donna e del Bambino

CORSO DI DOTTORATO DI RICERCA IN: Medicina dello Sviluppo e Scienze della Programmazione Sanitaria

CURRICOLO: Emato-Oncologia, Genetica, Malattie Rare E Medicina Predittiva

Ciclo 30°

**TISSUE ENGINEERING FOR THE SURGICAL TREATMENT OF MUSCLE DEFECTS:  
APPLICATION ON ANIMAL MODEL OF CONGENITAL DIAPHRAGMATIC HERNIA  
AND SKELETAL VOLUME MUSCLE LOSS**

**Coordinatore:** Ch.mo Prof. Carlo Giaquinto

**Supervisore:** Ch.mo Prof. Piergiorgio Gamba

**Co-Supervisore:** Dott.ssa Michela Pozzobon

**Dottorando :** Alberto Sgrò

# Summary

❖ <b>Abstract</b> .....	page 1
❖ <b>Introduction</b> .....	page 3
➤ Skeletal Muscle Anatomy.....	page 3
➤ Muscle Regeneration.....	page 4
➤ Extracellular Matrix.....	page 8
➤ Tissue engineering of skeletal muscle.....	page 11
➤ Decellularization of tissues for ECM-scaffold production.....	page 13
❖ <b>Aim of the Study</b> .....	page 16
❖ <b>Materials and Methods</b> .....	page 18
➤ Animals.....	page 18
➤ Tissues decellularization.....	page 18
➤ DNA extraction.....	page 19
➤ DNA quantification.....	page 19
➤ DNA gel electrophoresis.....	page 20
➤ ECM component quantification.....	page 20
➤ Freezing process.....	page 22
➤ Microscopes and Imaging Systems.....	page 22
➤ Immunofluorescence.....	page 22
➤ Histology.....	page 23
➤ In vivo implantation.....	page 24
➤ RNA extraction and PCR analyses.....	page 27
➤ Statistical analyses.....	page 28

❖ <b>Results</b> .....	page 29
➤ Analysis of decellularized scaffolds.....	page 29
➤ Results of in vivo application.....	page 34
▪ <i>Skin and Intestine ECM implanted on diaphragm</i> .....	page 34
• <i>Immunofluorescence and histologic analysis of application on diaphragm</i> ...	page 34
▪ <i>Volume Muscle Loss model</i> .....	page 35
• <i>Histological analysis</i> .....	page 35
• <i>Immunofluorescence and qRT-PCR</i> .....	page 37
❖ <b>Discussion</b> .....	page 41
❖ <b>Conclusions</b> .....	page 46
❖ <b>Bibliography</b> .....	page 47

# Abstract

**Background.** Repair of skeletal muscle loss due to trauma, surgical resection or malformations represent a challenge for clinicians. Several attempts to create a bioscaffold to substitute skeletal muscle have been done but no satisfying results were obtained due to lack in regeneration process and functionality of repaired tissue. Some studies on tissue engineering investigated the application of decellularized extracellular matrix (ECM) derived from skeletal muscle observing positive effect towards regeneration. It is becoming relevant the role of tissue-specificity in the field of tissue engineering. This study aims to compare the regenerative effect of both tissue-specific and no tissue-specific scaffolds when applied in a volume of volume muscle loss. Muscle regeneration and macrophagic response are investigated.

**Material and Methods.** Decellularized extracellular scaffold from murine skin, intestine and rhabdomyosarcoma (ARMS) were obtained using a detergent-enzymatic protocol. Scaffolds' characteristics were investigated. Wild type mice were used as animal model for in vivo implantation on diaphragm and tibialis anterioris muscles. Samples were obtained at sequential timepoints and analysed with Histology, DNA quantification techniques, Immunofluorescence, Real-time PCR.

**Results.** Decellularized ECM scaffold were obtained from each tissue. Moreover, their ECM maintained ultrastructure and composition. Implantation in vivo showed a regeneration of new, centre nucleated myofibers when muscle scaffold was used. No significant regeneration was observed with other scaffolds. With muscle implants, macrophagic response was present and characterized by organized distribution of cells.

**Conclusions.** The decellularization protocol used in this study demonstrated to be effective in maintaining ECM properties even if in absence of cells. Pro-regenerative

results obtained only with implantation of muscle-derived scaffolds underline the importance of tissue-specificity in order to obtain the ideal material to repair muscular defects.

# **Introduction**

Skeletal muscle is one of the most represented tissue in human body, it is a contractile tissue that allows movements through tendons attached to the bones.

Skeletal muscle injuries and defects have different origins. Congenital malformations, degenerative conditions, traumas and extended surgical resections may lead to a significant loss of muscle mass and functionality, when the loss is more than 20% is termed volumetric muscle loss (VML).

In VML the innate regenerative potential of the muscle, efficient in repairing small wounds, is lost and mechanisms leading to regeneration are limited giving rise to an hypotrophic muscle with impaired functionality.

The current standard of care for VML is autologous replacement transferring muscle tissue from a donor site of the same patient. In other cases, such as in congenital malformations with absent muscle portion, the defect is repaired using prosthetic patches of different materials. In all cases there is always a loss in muscle strength and functionality due to scar formation and lack in regeneration of real contractile tissue.

Tissue engineering is a new frontier in treatment of skeletal muscle diseases. It aims to stimulate regeneration of muscle tissue to reach volume, structure and functionality close to the original condition.

## **Skeletal muscle Anatomy**

A whole skeletal muscle is composed by hierarchical composition of elements which are coordinated during contraction. Contracting cells composing muscles are the myofibrils.

The contractile unit of myofibrils is the sarcomere which consists of interposing filaments of actin and myosin. A group of myofibrils form the so called myofibers that is the

structural basis of muscle. Similarly, myofibers forms a larger bundle inside the muscle called fascicles. At extremities skeletal muscle prolongates towards strong connective tissue forming tendons. These represents the connection between contractile tissue and the skeleton segments.

Skeleton muscle is not only formed by contractile cells and structure, indeed inside muscle mass there are several components fundamental to its functionality and maintenance such as blood vessels and nerves that form a complex and extended network between subunits of muscle allowing adequate perfusion and regulating contraction respectively.

An important role in muscle anatomy is also played by non-cellular elements. Each myofiber is surrounded by a basement membrane called basal lamina that is composed by fibronectin, type IV collagen, laminin and other proteins. Basal lamina acts as fundamental guide in the mechanism of endogenous tissue regeneration. Extracellular matrix (ECM) is the structure surrounding myofibers and it plays an important role in maintaining integrity of muscle and giving fundamental stimuli during reparative and regenerative processes. ECM is composed by several molecules of which most important are glycosaminoglycans, proteoglycans, collagen, fibronectin, lamin.

Finally, between myofibers and basal lamina muscle stem cells are present, the so called satellite cells (SC). In healthy and mature muscle they are quiescent and they are the primary cell type responsible of muscle regeneration in case of damage.

## **Muscle Regeneration**

Basis of muscle regeneration are similar to those of muscle development. Muscle development program is reactivated towards reconsruction when a tissue injury or volume loss occurs [1]. Satellite cells are committed toward regeneration, from the quiescent

satellite cells to the more fully differentiated muscle cells as shown in fig. 1. Satellite cells reside between the basal lamina and sarcolemma forming niches and remaining quiescent until their recruitment for formation and reparation of myofibers [8, 9]. Satellite cells can be activated both by physiological stimuli (such as exercise) or muscular damage. They express Pax7 transcription factor which induce the expression of others transcription factors (MyoD, Myf5, Myogenin, and MRF4) involved in the myogenic program. The activation of MyoD and Myf5 is fundamental for the formation of mature muscle cells [2].

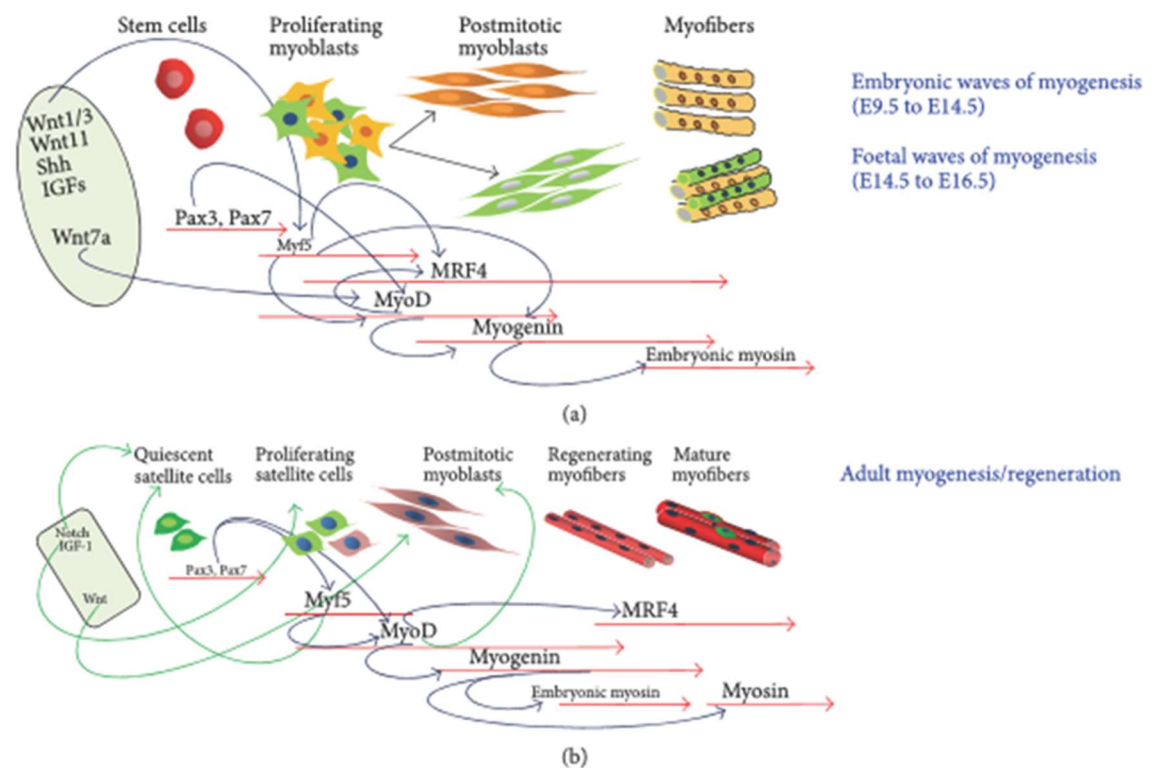


Fig. 1. From A Musarò. The Basis of Muscle Regeneration. Advances in Biology. Volume 2014. Article ID 612471.

Regeneration process after a muscular injury consists of different phases strictly inter-related. These phases can be resumed in *degeneration, inflammation, regeneration, remodelling and maturation* (fig. 2).

*Degeneration.* Necrosis of damaged myofibers produces debris and degradation elements which stimulate an inflammatory response. *Inflammation* plays a fundamental role in the equilibrium of the whole regenerative process and specific myeloid cells are recruited [3]. Neutrophils are the first cells to reach the damage site and they are detectable during first 24 hours. They have a phagocytic activity during which pro-inflammatory cytokines and free radicals and protease are secreted [3, 4]. These molecules stimulate the homing of monocytes and macrophages at the site of injury. Macrophages are the most represented inflammatory cells and they can be found at the level of perimysium and epimysium. Their role is to eliminate the debris and to activate stem cells towards differentiation and maturation [5, 6]. There are two types of macrophages. Type 1 inflammatory macrophages (M1) are present during phases of phagocytosis and debris elimination. After that they switch into type 2 anti-inflammatory macrophages that are fundamental for the maintenance of an adequate environment for regeneration (M2) [5, 7].

Satellite cells play a key-role as stem cells in the phase of *regeneration*. After activation, they form myoblasts that will fuse with damaged myofibers or will generate new real myofibers. A small part of activated satellite cells remains undifferentiated and, after proliferation, re-enter quiescent phase to maintain the pool [10]. Myf5 is detectable in proliferating cells not committed to differentiation. Depending on MyoD expression proliferating cells may follow two different lines. Cells expressing MyoD downregulate Pax7 and activate myogenin expression towards differentiation. On contrary, the downregulation of MyoD drives the proliferating cells into the self-renewal cycle to maintain the stem cells pool [11, 12, 13].

Other non-muscle cells have been demonstrated to participate in regeneration. Endothelial associated cells, interstitial cells and bone marrow-derived cells involved in regenerative process can reside among myofibers or they can be recruited from bloodstream via homing signals. [14, 15, 16, 17].

There are specific interstitial cells, called fibro-adipocyte progenitor (FAP), which are quiescent while in contact with intact myofibers. After injuries in physiologic conditions they participate in muscle repair through paracrine factors and satellite cells-mediated regeneration. On the contrary, in degenerative disease or in extensive tissutal disruption, they turn into fibro-adipocyte committed to fat and fibrosis deposition responsible of muscle dystrophy [18, 19].

*Remodelling.* Last phases of regeneration is remodelling of connective tissue with angiogenesis, and innervation to obtain the definitive maturation and functional repair. A key role during these phases is played by extracellular matrix. Regenerating tissue is stabilized by the production of structural molecules such as proteoglycans, collagen, fibronectin, elastin, laminin which re-organize into a scaffold driving the correct disposition of new myofibers, blood vessels and nerves [20]. Normal functionality of regenerated muscle is strictly dependent on innervation and this is especially relevant during last steps of regeneration. Indeed, within two weeks of damage new neuromuscular junctions can be identified and their activity can influence proliferating and maturing myofibers and their production of new myotubes. Satellite cells activity in regeneration has also been showed to be influenced by nerves activity [21, 22]. Extracellular matrix and its fundamental role in regeneration process and angiogenesis represent the main topic of this thesis and it will be widely discussed.

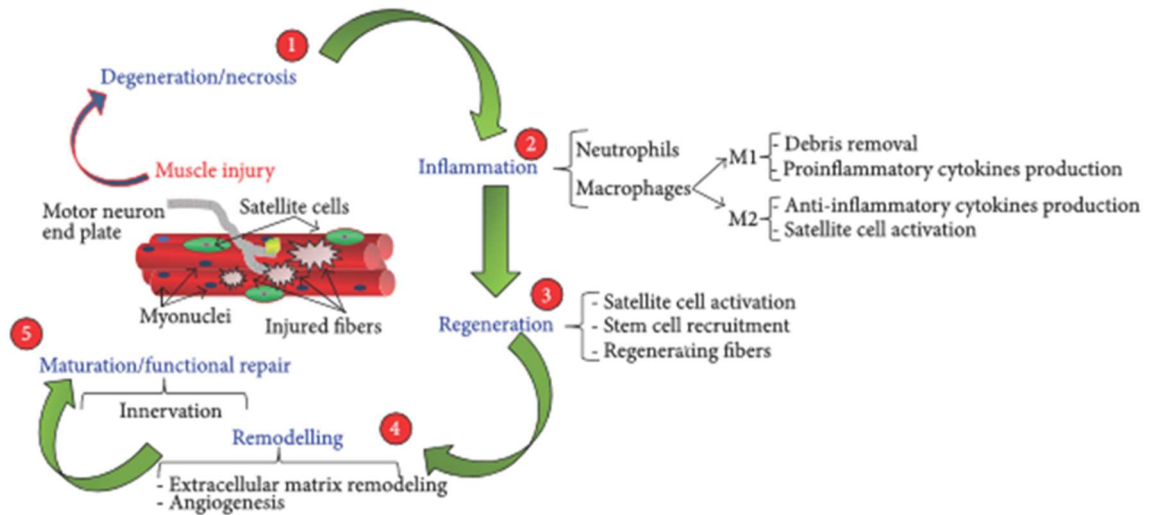


Fig. 2. Summary of different phases of regeneration process. From A Musarò. The Basis of Muscle Regeneration. Advances in Biology. Volume 2014. Article ID 612471.

## Extracellular matrix

Extracellular matrix (ECM) is a complex structure surrounding and supporting cells forming a tissue (Fig. 3). It has a three-dimensional architecture and it is composed by different molecules among which most relevant are glycosaminoglycans (GAGs), glycoproteins, collagen, elastin, laminin and fibronectin. Disposition of these molecules varies among different tissues implicating that ECM structure is specific and different among tissues and organs [23, 24].

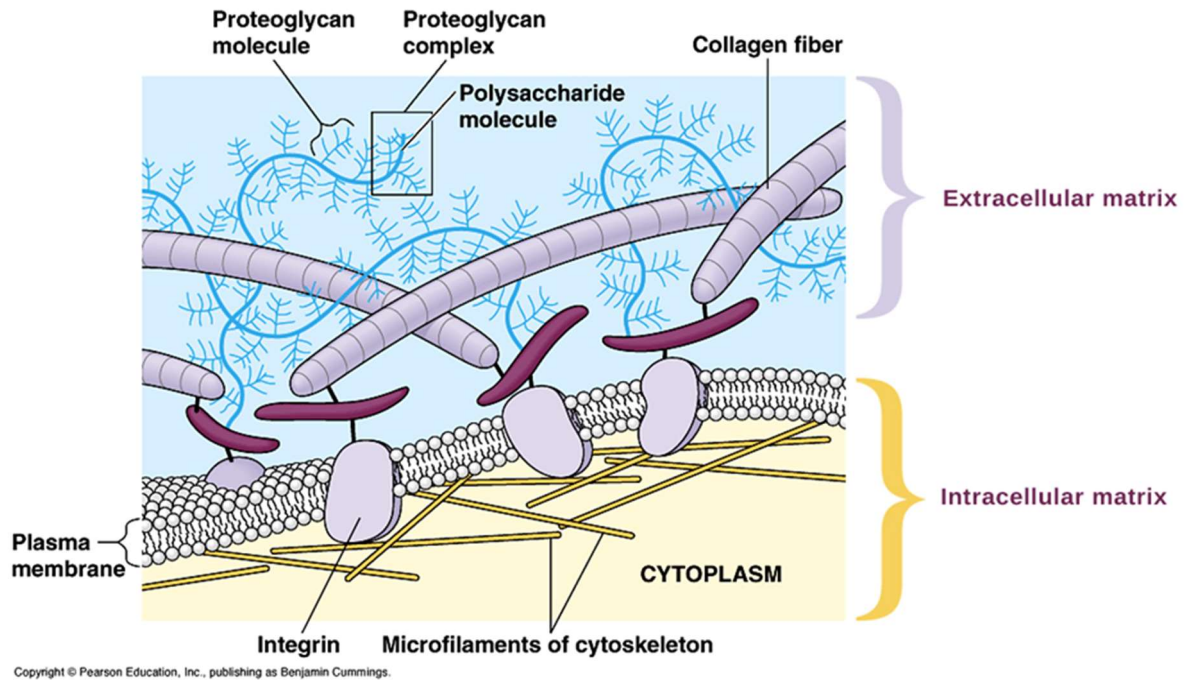


Fig. 3. Schematic representation of extracellular matrix and interactions with cells.

Collagen is present in the whole body as 20 or more subtypes but the most represented is Type I which is especially implicated in tendinous and ligamentous structure. Other frequent types of Collagen are Type III, IV, VI, and VII and they all provide structural strength [23]. Collagen arranges with glycoproteins, laminin and fibronectin into three-dimensional structures. Fibronectin is another ECM component widely represented and it plays an adhesion role connecting to integrins on cellular surface. Laminin plays a role similar to fibronectin but it is also essential for formation and maintenance of vascular structures. GAG's type mostly detectable are chondroitin sulfate A and B, heparin, and heparan sulfate. They are responsible for water retention and gel function of ECM. They also bind growth factors and cytokine. [23]

Bioactive soluble cytokines and growth factors among structural molecules are fundamental for the modulation of cell behaviour. The most represented are fibroblast growth factor (FGF), epithelial growth factor, transforming growth factor beta (TGF-

beta), keratinocyte growth factors, hepatocyte growth factor (HGF), platelet derived growth factor (PDGF), and vascular endothelial growth factor (VEGF) [23].

Composition of many of the molecules described above is conserved through different species so that xenogenic ECM can be used for regenerative purpose avoiding the risk of rejection by the host. To be underlined is the different spatial and architectural disposition of molecules in ECM of different tissues. Even if components are similar, disposition and architecture are defined for each tissue. This aspect is fundamental when a regenerative purpose is intended. Indeed, architecture drives cells behaviour that can be different among tissues [24, 25, 26]. Moreover, architecture is the base of mechanical properties of the tissue, such as stiffness that has been shown to influence cell fate during differentiation [27, 28].

ECM is a dynamic structure that can influence proliferation, survival, migration and differentiation of cells. It is always under constant remodelling and this is much important for development but also regeneration and repair of a tissue such as muscle [30]. There are several receptors having a role in signalling during ECM remodelling such as integrins, Laminin receptors, syndecans. Several modifying enzymes are involved in the process of remodelling. Metalloproteinases with other protease dissolve ECM molecules through their proteolytic activity. Peptides and growth factor are released and acts as further signals driving regeneration [30]. These are further demonstration of the fundamental role of ECM in tissutal homeostasis, a process called “dynamic equilibrium” [23].

When ECM is irreversibly altered by diseases or damage, the equilibrium is lost leading to a leak in regenerative and remodelling processes [29].

Due to its properties in leading and stimulating regeneration, ECM has been investigated and applied for therapeutic purposes. ECM scaffolds derived from the porcine small intestinal submucosa (SIS), human dermis (Alloderm®) and urinary bladder have been

involved in reparation of vessels, skin and lower urinary tract. When applied to damaged organs a progressive reabsorption of the scaffold together with a significant tissutal regeneration were observed [30, 23, 31]. Skeletal muscle ECM, which is involved in the aim of this thesis, has also been investigated in several studies. ECM derived Tibialis Anterior of a mouse has been demonstrated to stimulate regeneration when implanted into the same muscle which had undergone a wide damage. After 2 weeks from implantation, regeneration of myofibers expressing muscle-specific proteins (myosin heavy chain and sarcoglycan) was observed. The presence of ongoing regeneration was also demonstrated by the presence of abundant cytoplasm and central nuclei in myofibers [32].

As seen above the structure of ECM is very complex and tissue-specific. The reconstruction of artificial ECM starting from single elements would be really difficult. For this reason, ECM are usually derived from decellularization processes to be used as biologic scaffold in tissue engineering. This way the native ECM and its structure are maintained while cellular components responsible of possible rejection are eliminated [23, 29, 25].

## **Tissue engineering of skeletal muscle**

Tissue engineering aims to reproduce *ex vivo* tissues and organs to obtain optimal substitute in case of traumatic damages or degenerative diseases. Some clinical experiences have already reported with skin, cartilage, vascular grafts, bones and other organs [33]. Due to its intrinsic complexity, tissue engineering of skeletal muscle is challenging. Several attempts to recreate muscle through artificial scaffold have been done. Structures made of matrigel [34], collagen [35, 36], fibrin [37] were created to support regeneration and remodelling of myofibers into new functioning contractile

muscle. Even if these artificial scaffold acts as a positive support for growth and differentiation of muscle precursor cells, the specific three-dimensional architecture and arrangement of all types of molecules in ECM has already been described as fundamental in determining growth and fate of cells. As seen previously, the whole ECM is, indeed, the specific product of cellular components of tissues supporting their phenotype and function through special and chemical signalling. For these reasons, the ideal bioscaffold for skeletal muscle is decellularized ECM obtained from native tissue of a donor. The ideal result should be a three-dimensional structure preserving physical and mechanical properties, maintaining tissutal homeostasis and supporting cell-matrix interactions [38]. Xenogenic ECM for muscle regeneration have been obtained from porcine small intestinal submucosa (SIS) and porcine urinary bladder mucosa (UB). These scaffolds have been well characterized [39, 40].

Porcine SIS is composed primarily by type I collagen, but also elastin and collagen types III, IV, and VI. In SIS glycoproteins such as fibronectin and laminin, glycosaminoglycans and proteoglycans are present mediating cell adhesion and attachment to the ECM. In addition, capability to bind growth factors and to retain enzymes has been observed. SIS represent a good biomaterial for muscle tissue engineering, thanks to its size, membranous configurations, uniformity, and availability. SIS has been clinically used to repair inguinal hernia and large abdominal wall defects, urinary tract, tendons, musculotendinous structures, vessels, and dermal wounds [41-46].

From porcine UB two ECM bioscaffold can be derived: from tunica mucosa including basement membrane and from tunica sub mucosa. UB-ECM has been demonstrated to retain several growth factors among which VEGF, TGFbeta, PDGF, and basic fibroblast growth factor seem to mainly contribute to the regenerative potential of the scaffold. In addition to regeneration and healing, UB is characterized by antimicrobial properties [47-49]. Moreover, a prevalence of M2 macrophages in UB-ECM post-implantation period

has been observed and it is relevant to reduce scar deposition and enhance functional tissue regeneration [50].

Differently from SIS and UB, scaffolds derived from skeletal muscle are less characterized and they are now involved in some studies. As stated previously, it is evident that muscle tissue engineering needs a scaffold preserving composition of three-dimensional structure in which the correct parallel alignment of myofibers and the maintenance of mechanical properties becomes fundamental for function of the regenerated tissue. The first of few studies describing muscle-ECM properties is that from Perniconi [51]. They demonstrated that the scaffold provides the correct support for myofibers development and the appropriate architecture for muscle fiber formation. When implanted *in vivo*, the activation of myogenic process and the formation of new myofibers in areas within the bioscaffold were observed even if the grafts had almost completely degraded after 4 weeks.

Other authors demonstrated also that, after decellularization, muscle ECM retains collagen and GAGs composition, the overall architecture of the native ECM, same mechanical properties, and the capability to sustain myogenic cells [52].

## **Decellularization of tissues for ECM-scaffold production**

As seen in previous chapters the ideal bioscaffold for tissue engineering seems to be the native acellular ECM of the organ, especially for skeletal muscle regeneration. To obtain ECM, decellularization technique becomes fundamental. Through decellularization a complete removal of cells from ECM is obtained while three-dimensional architecture, mechanical and chemical properties are preserved [53]. Major histocompatibility complexes I and II and nucleic acids of cells are responsible of individual specificity and, as consequence, of the probable immune-mediated rejection of a graft. For this reason,

removal of cellular components is important for a correct integration of the scaffold. In order to obtain pro-regenerative ECM scaffold, several decellularization techniques have been developed depending on the characteristics of the tissue, such as size, cellularity, density and thickness [54].

Treatments can be physical, enzymatic or chemical, or a combination of them. Physical methods include mechanical agitation, freeze/thaw, pressure, electroporation and sonication. Enzymes usually employed are trypsin, dispase and endo/exonucleases. Chemically it is possible to use alkaline/acid or hypotonic/hypertonic solutions, but also chelating agents such as ethylene diamine tetraacetic acid (EDTA) or ethylene glycol tetraacetic acid (EGTA). Furthermore, several types of detergents can be used, such as the non-ionic Triton X-100, the ionic ones sodium dodecyl sulfate, Triton X-200, sodium deoxycholate (SDC) or the zwitterionic CHAPS, Sulfobetaine-10 and -16 or tributyl phosphate (TBP) [53, 54].

Tissue and organs can undergo decellularization treatments through the whole organ perfusion or the immersion with agitation. Perfusion through vasculature is very efficient as it allows a wide delivery of the agents to remove cells and debris. Perfusion can be applied to big organs such as heart [55], lungs [56], and liver [57] but it is not suitable for little tissues. Portion of skeletal muscle can not be perfused so the immersion in decellularizing solutions and gentle agitation is used [52]. Such technique has also been used for several others tissues, for example heart valves [58], blood vessels [59], tendons [60], trachea [61], oesophagus [62], dermis [63], and urinary bladder [40].

Different criteria have been established to assess if the decellularization could be considered acceptable: the amount of dsDNA is less than 50 ng per mg of ECM (dry weight); there is not visible nuclear material in tissue sections stained with DAPI or hematoxylin and eosin (H&E); the remaining DNA fragments have a length less than 200 bp [54]. Furthermore, the maintenance of three-dimensional ultrastructure, composition,

and mechanical properties of ECM should be assessed after decellularization process. Scanning electron microscopy or transmission electron microscopy are usually employed to investigate the structure, while histological evaluations (H&E, Masson's Trichrome, Elastic Van Gieson, Alcian Blue) and protein quantifications are useful for assessment of the composition of ECM, especially of Collagen, elastin and GAG's. The presence of soluble factors such as cytokines, growth and angiogenic factors may be analysed using spectrometry. Most used parameters to evaluate mechanical properties are stiffness and elastic modulus [54, 64].

The conception of a new ECM-derived bioscaffold should pass through the assessment and choice of the best decellularization technique and process for that specific tissue.

## Aim of the study

In the introduction, an overview on the complex muscle regeneration process has been provided underlining the need for a bioscaffold capable to induce the production of muscle with normal structure, but also normal functionality.

My PhD project has been developed at the Regenerative Medicine Lab of the Paediatric Institute of Research in Padova (Italy). The project is strictly connected to previous studies from this group. In particular, the group had previously developed an ECM scaffold of murine diaphragm through a detergent-enzymatic decellularization process. Once implanted in vivo in a murine model, scaffold effect for regenerative purposes was observed. The results have been published by Piccoli et al. in 2016 [65]. They demonstrated for the first time that *“orthotopic transplantation of a decellularized diaphragmatic muscle from wild animals promoted tissue functional recovery in an established atrophic mouse model. In particular, ECM supported a local immunoresponse activating a pro-regenerative environment and stimulating host muscle progenitor cell activation and migration. These results indicate that acellular scaffolds may represent a suitable regenerative medicine option for improving performance of diseased muscles”*.

Following these results, further investigations on development of muscular acellular ECM scaffold were planned and carried out in this PhD project.

The aims of the study are:

- To investigate the efficacy of the same decellularization protocol when applied to tissues different from muscle (skin, intestine). Pathologic muscle (rhabdomyosarcoma) was also investigated.
- To investigate the regenerative effect of acellular ECM of different tissues (skin, intestine) when applied on diaphragm. Moreover, the macrophagic population

(M1 and M2) is investigated to obtain data about immuneresponse elicited by these scaffolds.

- To investigate the regenerative effect of acellular ECM derived from muscle and different tissues (skin, intestine, rabdomiosarcoma) in a murine model of Volume Muscle Loss.

# Materials and methods

## Animals

All surgical procedures and animal husbandry were carried out in accordance with University of Padua's Animal care and the Ministry of Health (protocol number 862/2016-PR and 304/2017) in accordance with the Italian Law on the use of experimental animals (DL n. 16/92 art. 5). The animals used as donors (quadriceps, skin, intestine for scaffold generation) were 12 week-old wild type C57BL/6j male and female; 12 week-old C57BL/6j mice were used also as recipients.

For xenogenic Alveolar Rhabdomyosarcoma production,

Balb/c Rag2<sup>-/-</sup> gamma c<sup>-/-</sup> mice from Jackson laboratories were used to grow xenograft of alveolar rhabdomyosarcoma tumors after injection in flanks of RH30 cell line. Mice were 12 week-old, male and female.

## Tissues decellularization

The decellularization was obtained using a detergent enzymatic treatment (DET) [65], in which both chemical agents and enzymes were employed. Specifically, 4% SDC (Sigma-Aldrich) was used as detergent and deoxyribonuclease I (DNaseI) (Sigma-Aldrich) as enzyme. *Quadriceps muscles, skin and intestine* samples were cut in half and then washed in sterile 1X PBS. A DET cycle consists of 3 passages. First, the quadriceps were maintained in 40 mL of sterile and deionized water at 4° C for 24 hours. Then, the samples were put in 40 mL of 4% SDC for 4 hours at RT and in gentle agitation. After that, samples were washed 3 or 4 times with sterile and deionized water, to remove the detergent that could inhibit the DNase I (or could be toxic for cells if the scaffold will be recellularized or implanted in vivo). At last, the tissues were put in 40 mL of 2000 kU DNaseI (Sigma-Aldrich) in 1 M NaCl (Sigma-Aldrich) for 3 hours at RT and in gentle

agitation. Then, another cycle started. After decellularization, matrices were rinsed for at least 3 days in 1X PBS with 3% P/S (Gibco-Life Technologies), immediately analyzed or stored in freezing medium composed of 70% FBS, 20% DMSO, 10% DMEM high glucose and frozen in liquid nitrogen.

*Rhabdomyosarcoma decellularization.* The detergent used was 1% SDS (Sigma-Aldrich) and the procedure was the same as described above.

## **DNA extraction**

To assess total DNA content within the native fresh and decellularized tissues, specimens were treated using DNeasy for blood & tissues (Qiagen). Samples (up to 25 mg tissue) were first lysed overnight using proteinase K and buffer ATL. After lysis, 200  $\mu$ L of absolute ethanol were added to provide optimal DNA binding conditions and the lysate was loaded onto the DNeasy Mini spin column. During centrifugation at 8000 rpm for 1 minute, DNA is selectively bound to the DNeasy membrane as contaminants pass through. Remaining contaminants and enzyme inhibitors are removed by washing with buffers AW1 and AW2. After the addition of each buffer, tubes were centrifuged at 14000 rpm for 3 minutes. DNA was then prepared for elution by adding buffer AE, left to act for 1 minute. Columns were then centrifuged at 8000 rpm for 1 minute in a new tube, in which nucleic acids were eluted.

## **DNA quantification**

DNA extracts were evaluated using Nanodrop 2000 (Thermo scientific, USA). Nucleic acids have an absorption maximum at 260 nm. Most samples contain contaminants such as proteins and single stranded DNA/RNA that absorb maximally at 280 nm. Hence,

optical densities at 260 nm and 280 nm were used to estimate the purity and yield of nucleic acids, which were quantified on the basis of 260 nm absorbance.

## **DNA gel electrophoresis**

To verify whether the DNA found in extracts from tissues after each DET cycle was genomic or only composed by fragments retained in the matrix, a gel electrophoresis was performed. 33  $\mu\text{L}$  out of 100  $\mu\text{L}$  of DNA extracted from samples were taken and resuspended with 8.25  $\mu\text{L}$  of loading buffer. 20  $\mu\text{L}$  of each sample was loaded in a 0.8% Agarose in TBE 1X gel, in which we added 8  $\mu\text{L}$  of SybrSafe, a reagent that binds to DNA and allows its visualization when exposed to UV light. Gel electrophoresis run was done at 110 V for 90 minutes.

## **ECM component quantification**

### *Collagen quantification*

The collagen content of fresh and decellularized tissues was quantified using the SIRCOL collagen assay (Biocolor, UK) according to the manufacturer's instructions. The samples were incubated overnight at 4° C with 1 mL of 0.5 M acetic acid containing 0.1 mg of pepsin, to remove the terminal non-helical telopeptides and release the collagen into solution. Extracts were then incubated overnight at 4° C with Acid Neutralising Reagent (contains TRIS-HCl and NaOH) and Collagen Isolation & Concentration Reagent (contains polyethylene glycol in a TRIS-HCl buffer, pH 7.6). After this step, samples were centrifuged at 12000 rpm for 10 minutes, supernatant was removed, and samples were incubated 30 minutes in a mechanical shaker with Sirius red dye. Samples were centrifuged again at 12000 rpm for 10 minutes, supernatant was removed and Acid-Salt Wash Reagent (containing acetic acid, sodium chloride and surfactants) was added to

remove unbound dye from the surface of the pellet and the inside surface of the microcentrifuge tube. A final centrifugation step at 12000 rpm for 10 minutes was done and supernatant was removed. Alkali reagent (contains 0.5 M sodium hydroxide) was added and tubes were vortexed to release Sircol dye from the collagen-dye complex. A volume of 200  $\mu$ L of each sample was transferred into a 96 well microplate and Absorbance was determined at 555 nm with a microplate reader (Biorad). Reading was made at this absorbance because the spectrum chart of the Sircol Dye in Alkali Reagent has a peak maximum in the visible region of 555 nm. Aliquots containing 50, 25, 12.5, 6.25 and 0  $\mu$ g of the Collagen Reference Standard (made of Collagen I extracted from bovine skin) were used to create a standard curve with which it was possible to calculate the collagen content of the different fresh or decellularized samples.

#### *Glycosaminoglycans quantification*

The sulfated glycosaminoglycans (sGAG) content of fresh and decellularized tissues was quantified using the Blyscan GAG Assay Kit (Biocolor, UK). 50 mg of wet fresh or decellularized tissue were weighed and placed in a microcentrifuge tube containing 1 mL of Papain Extraction Reagent: 0.2 M sodium phosphate buffer ( $\text{Na}_2\text{HPO}_4 - \text{NaH}_2\text{PO}_4$ ) at pH 6.4, 0.1 M sodium acetate, 0.01 M  $\text{Na}_2\text{EDTA}$ , 0.005 M cysteine HCl, 15-20 mg of papain, and incubated in a water bath at 65° C for 3 hours. Samples were then centrifuged at 10000 rpm for 10 minutes and supernatant was decanted off. Each sample was incubated for 30 minutes in a mechanical shaker with Blyscan dye (contains 1,9-dimethylmethylene). Samples were centrifuged at 12000 rpm for 10 minutes, supernatant was carefully removed and dissociation reagent was added (contains the sodium salt of an anionic surfactant) to dissociate the sGAG-dye complex and enhance the spectrophotometric absorption profile of the free dye. A volume of 200  $\mu$ L of each sample was transferred into a 96 well microplate and Absorbance at 656 nm was measured using

a microplate reader (Biorad). Reading was made at this absorbance because the spectrum of the Blyscan Dyein the Dissociation Reagent has a peak maximum of 656 nm. A standard curve was set up using GAG standards containing 1, 2, 3, 4 and 5  $\mu\text{g}$  of bovine trachealchondroitin-4-sulfate, to determine the GAG content.

### **Freezing process**

All the tissue samples were fixed with 4% PFA for 1 hour at 4° C. Then, they were dehydrated with a sucrose gradient (10%, 15% and 30%) (Fluka), in order to maintain the original structure of the tissue. At last, they were included in the cryostat embedding medium O.C.T. (Kalttek) and frozen in liquid nitrogen using isopentane (Sigma-Aldrich). The frozen tissues were sectioned with cryostat (Leica CM1520) in sheets of 6-7  $\mu\text{m}$ .

### **Microscopes and imaging system**

Phase-contrast images were collected using an inverted microscope (Olympus IX71). Immunofluorescence analyses were performed using a fluorescence inverted microscope (Leica B5000).

### **Immunofluorescence**

Tissue slides (both from the in vivo and in vitro experiments) were permeabilized with 0.5% Triton X-100 in 1X PBS for 10 minutes at RT. After, the samples were rinsed in 1X PBS for 5 minutes and then saturated with 5% HS in 1X PBS for 12 minutes and with mouse serum in 1X PBS (dilution 1:10, Sigma-Aldrich) for 30 minutes at RT. Another washing step in 1X PBS for 5 minutes was done. Samples were then incubated with primary antibody for 1 hour at 37° C or overnight at 4° C. After a washing step with 1X PBS, they were incubated with labeled secondary antibody for 1 hour at 37° C. After the last

washing step with 1X PBS, nuclei were counter stained with fluorescent mounting medium plus 100 ng/mL 4',6-diamidino-2-phenylindole (DAPI) (Sigma-Aldrich).

Antibodies used for immunofluorescence are summarized in table 1.

<b>Primary Antibodies</b>	<b>Manufacturer</b>	<b>Dilution</b>
rabbit anti-mouse Myf5	Santa Cruz	1:80
rabbit anti-mouse Ki67	Abcam	1:100
rabbit anti-mouse Laminin	Sigma-Aldrich	1:200
rat anti-mouse Laminin	Santa Cruz	1:80, with over night incubation
mouse anti-human PAX7	R&D Systems	1:50
mouse anti-human Lamin A/C	Leica	1:100
rabbit anti-mouse Collagen type 1	Thermo Scientific	1:80
rabbit anti-human Cleaved Caspase-3	Cell signalling	1:300, with overnight incubation
mouse anti-human MyoD	Dako	1:80, with overnight incubation
mouse anti-mouse MYH3	Santa Cruz	1:100
rabbit anti-human Myogenin	Santa Cruz	1:100, with overnight incubation
<b>Secondary Antibodies</b>		
Alexa Fluor chicken anti-rabbit 594	Life Technologies	1:200
Alexa Fluor chicken anti-rabbit 488	Life Technologies	1:200
Alexa Fluor goat anti-mouse 594	Life Technologies	1:200
Alexa Fluor goat anti-rat 568	Life Technologies	1:200
Alexa Fluor goat anti-rat 488	Life Technologies	1:200

Tab 1: List of antibodies used for Immunofluorescence.

## Histology

Frozen sections (6-7  $\mu$ m thick) were stained with H&E kit for rapid frozen section, Alcian Blue, and with Masson's Trichrome (MT) with aniline blue kit (all from Bio-Optica, UK) under manufacturer's instruction.

## ***In vivo* implantation**

### *Orthotropic implantation on diaphragm*

Surgical procedure was carried as previously described. Briefly, while in a recumbent position, a medial incision was performed in the abdomen of the mouse. To visualize the diaphragm, liver and stomach were then gently moved aside with the help of a sterile gauze. Patches of skin and intestine (0,7x0,7 cm each) were fixed on the left side of the native diaphragm with stitches of Prolene 8/0. Organs were then repositioned into the abdominal cavity. The abdominal wall was closed in two layers and the animals were left to wake up under a heating lamp. Mice were euthanized by cervical dislocation at 7 and 15 days post implantation.

### *Implantation on tibialis anterioris muscle (VML model)*

C57BL/6j mice were used when surgical application of natural- derived scaffolds was performed. Surgery was performed in order to create a standardized murine model of TA VML injury for the application of biocompatible scaffolds (Fig 4). Mouse were gently handled in general anesthesia with O<sub>2</sub> and isofluorane (Forane, Merial, IT). The mid-belly region of TA muscle was visualized through a 0.5-1 cm incision longitudinally in the epidermis, dermis, and fascia. A 4 x 4 x 3 mm thickness segment was resected from muscle mass, and an average defect muscle mass of 25-30 mg was excised [66]. Defects were treated with size-matched biocompatible scaffolds:

1. Decellularized healthy quadriceps
2. Intestine decellularized extracellular matrix
3. Skin decellularized extracellular matrix
4. Alveolar rhabdomyosarcoma decellularized extracellular matrix

The scaffolds were hydrated using normal saline buffer before dermal closure with 7-0 prolene. The deep fascia and skin were closed using non-absorbable sutures [67]. Afterwards, the animals were checked to ensure arousal within 10 minutes after surgery and moved back to their cages monitored for activity, ability to drink and eat and for signs of bleeding or infection. Analgesics (as painkillers), antibiotics and saline solution (for rehydration) were administered. All animals survived the surgical procedure and study period without complications. Mice were euthanized by cervical dislocation at 7 and 15 days post implantation. List of treated animals is provided in table 2.

### Natural-derived

Scaffolds have been previously prepared, cut in 4 x 3 x 3 mm size using a biopsy punch of 5 mm, washed and weighed.

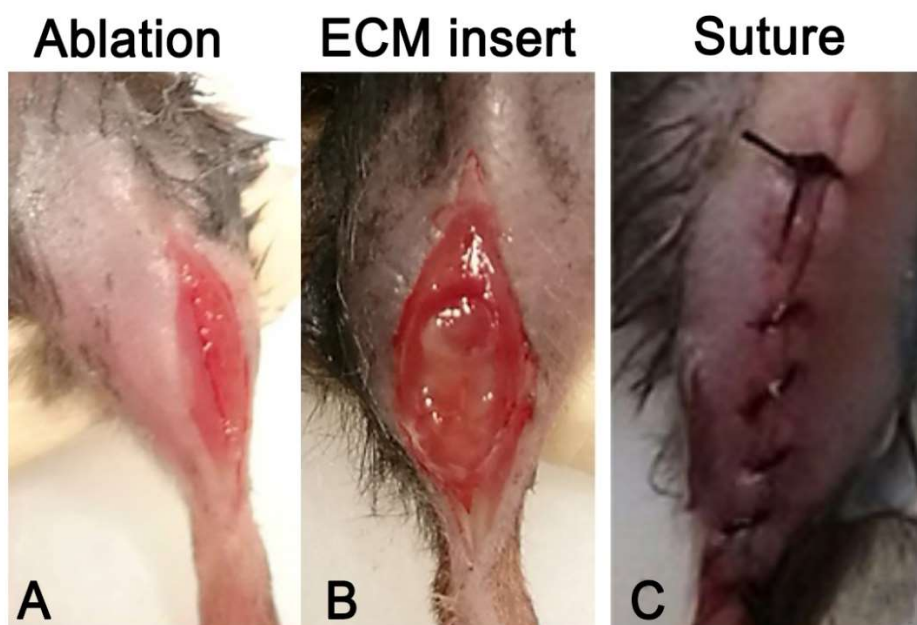


Figure 4: Surgical procedure for VML defect in TA muscle of a murine model (Fig. XXX): A) Middle incision and muscle resection to create the VML into the TA muscle. B) Application of biocompatible scaffolds. C) Closure of the treated TA muscle and skin.

Legend	QUADRICEP	INTESTINE	SKIN	ARMS
# mouse	Tibialis Anterioris Left		Tibialis Anterioris Right	
	Surgical resection (mg)	Weight of the scaffold (mg)	Surgical resection (mg)	Weight of the scaffold (mg)
1	30,5	38		
2	19	33		
3	18,5	30		
4	29,8	36		
5	21,4	30		
6	29,1	32		
7	23	35	25	39
8	33,3	34,5	22,7	35,8
9	22,8	38	22,1	32,5
10	29	38,8	22,5	32,3
11	17,2	31,9	20,7	30,6
12	29,6	34,5	29,8	36
13	22,2	33	20	32
14	20	31	16	30,9
15	23,8	35	24,6	39
16	21,7	35,5	20	37,5
17	25,1	24	23,9	30
18	24,3	24,7	16,8	29,9
19	21,7	28,9	19,8	31,2
20	22,2	26,5	19,8	30,2
21	28	24,2	32,2	31,7
22	30,2	29	26,5	33,2
23	18,6	32,1	21,1	27,5
24	24,9	31	30,7	33,1
25	13,8	33	19,7	29,4
26	19,8	24	17,3	31,5
27	20,4	28,7	15,6	23,3
28	14,7	23	18	21,3
29	19,9	22,5	16,5	26,7
30	29,4	34,1	21	27,1
31	26,5	29,5	24,8	28,4
32	24,2	24,6	18,6	26,7
33	24,9	34,3	18,7	34,3
34	25,9	32,2	25,8	32,6
35	18,8	34,8	23,3	35,3
36	24,9	34	28,8	34,2
37	21,9	34,1	34,6	36,8
38	19,6	33,7	28,7	35,1
39	21,5	35,6	18,7	34,3
40	12,3	35,6	23,3	34,2
41	25,8	37,2	18	33,3
42	18,8	23	16,2	27,1
43	16,6	34,7	18,9	34,1
44	25	24,1	23,6	26,3
45	27,5	24,1	31	25,5
46	20,5	26,5	20,6	23,2
47	28,8	21	25,9	18,5
48	19,7	26	19,5	21
49	21,1	27,5	20,8	25,8
50	19,4	25	18	25,3
51	17,8	25,3	16,4	24,6
52	18,4	22,4	15,7	21,9
53	17,7	25,7	14,4	24,2
54	17,5	22,8	19,6	23,3
55	16,1	20,7	16,1	24,4
<b>Avarage</b>	<b>22,5</b>	<b>29,9</b>	<b>21,7</b>	<b>29,8</b>

Tab. 2: Weight of the muscle surgical resections and subsequent implanted scaffolds.

## RNA extraction and RealTime PCR analyses

The RNA was extracted from TA, treated with quadriceps, intestine, skin and ARMS, at two time points (7 and 15 days). Samples were collected in 1 mL of Trizol and mechanically homogenized using Tissue Lyser (Qiagen), then 200  $\mu$ L of chloroform were added and the samples were mixed for 15 seconds. After 5 minutes at RT they were centrifuged at 4° C for 15 minutes at 13000 g in order to separate the aqueous phase from the organic one. From the aqueous phase the RNA was extracted with the RNeasy® Plus Mini Kit (QIAGEN®) and then quantified with a ND-2000 spectrophotometer (Thermo Scientific, Waltham, MA, USA). One  $\mu$ g of RNA was reverse transcribed using High Capacity Reverse Transcription kit (Applied Biosystems) following manufacturer's instructions.

Afterwards, RealTime PCR reactions were performed in order to analyze the expression of *Nos2*, *Arg1*, *Myog* and *Myh3*. Ribosomal RNA 18S was used as housekeeping gene. Table 3 shows the primer sequences, the annealing temperature and the length of the product for each gene.

RealTime PCR reactions were performed using a LightCycler II (Roche, Monza, Italy). Reactions were carried out in triplicate using 4  $\mu$ L of FASTSTART SYBR GREEN MASTER (Roche) and 2  $\mu$ L of primers mix FW + REV (final concentration, 300/300 nM) in a final volume of 20  $\mu$ L. Serial dilutions of a positive control sample were used to create a standard curve for the relative quantification. The amount of each mRNA was normalized over the expression of *18S*.

<i>Gene</i>	<i>Primers</i>	<i>T</i> (°C)	<i>Product</i> <i>length (bp)</i>
<i>Nos2</i>	FW: GCAGGTCTTTGACGCTCGGA RV: ATGGCCGACCTGATGTTGCC	60	105
<i>Arg1</i>	FW: AGACCACAGTCTGGCAGTTGG RV: AGGTTGCCCATGCAGATTCCC	60	136
<i>Myog</i>	FW: GCAATGCACTGGAGTTCG RV: ACGATGGACGTAAGGGAGTG	58	94
<i>Myh3</i>	FW: AGGCCTTGTGCTTTCCCAGAG RV: GTTCACAGCATGGTGAACCTGG	60	86
<i>18S</i>	FW: CAACTTCAATGTCGGATGGATG RV: GCTGTGCTCGCGCTACTCT	60	161

Table 3: RealTime PCR. Primers, annealing temperatures and length products of the cDNA amplified with the PCR. FW: forward; RV: reverse.

### Statistical analyses

Statistical analyses were performed with GraphPad Prism software 5. The data are presented as the mean  $\pm$  S.E.M. Differences between data groups were evaluated for significance using the unpaired Student's t-test. P-values indicated on figures are \* =  $p < .05$ ; \*\* =  $p < .01$ ; \*\*\* =  $p < .001$ .

# Results

## **Analysis of decellularized scaffolds**

In Fig. 5 and 6 structure and composition of decellularized skin and intestine are reported. After 3 Detergent-Enzymatic treatment cycles comparable results were observed for intestine and skin. Immunofluorescence for DAPI (cells nuclei) and laminin (ECM component surrounding cells) demonstrated that after 3 detergent enzymatic cycles the structure of cells remained but no nuclei were still visible. DNA quantification together with electrophoresis confirmed the significative absence of cellular remnants in the samples.

Histologic staining and quantification assay showed a substantial stability in collagen and GAGs distribution and quantity. After 3 cycles of Detergent-Enzymatic treatment the extracellular matrix structure and composition of skin and intestine was not significantly altered while a successful decellularization was achieved.

Qaudricep and ARMS scaffold obtained with the same decellularization protocol, have been investigated by authors of the same laboratory. Results demonstrated that also ECM scaffold from these tissues retains structural properties comparable to those of the fresh tissue. Results have been recently published by the authors [80, 81] and they are reported in Fig. 7, 8, and 9.

In particular for ARMS ECM the new detergent SDS instead of SCD was used to rich to decellularization efficiency.

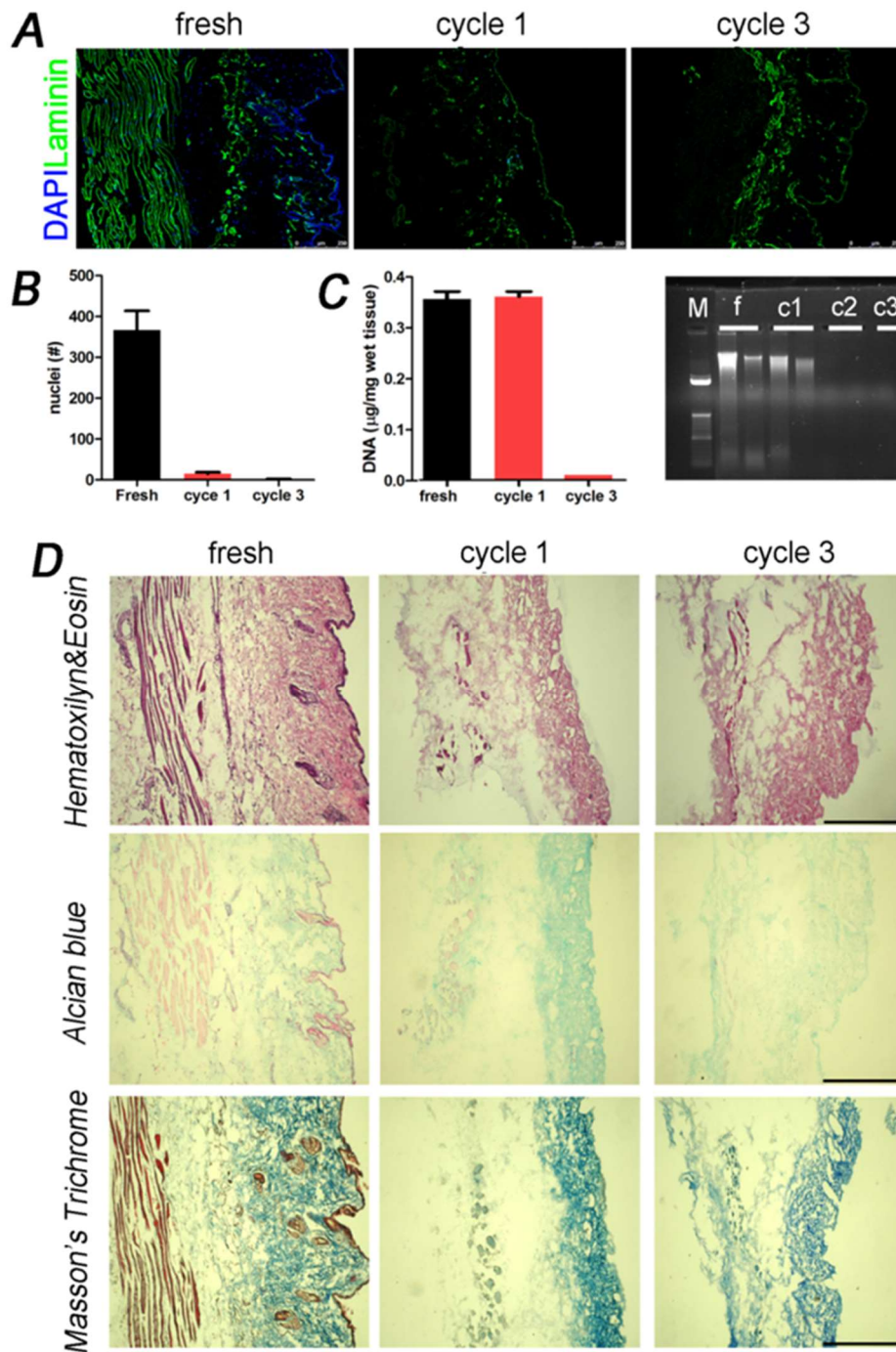


Fig. 5. Characterization of Skin ECM after decellularization. Results after 3 DET cycles. Immunofluorescence (A), Nuclei quantification (B), DNA quantification (C), and ECM Components (D) are reported.

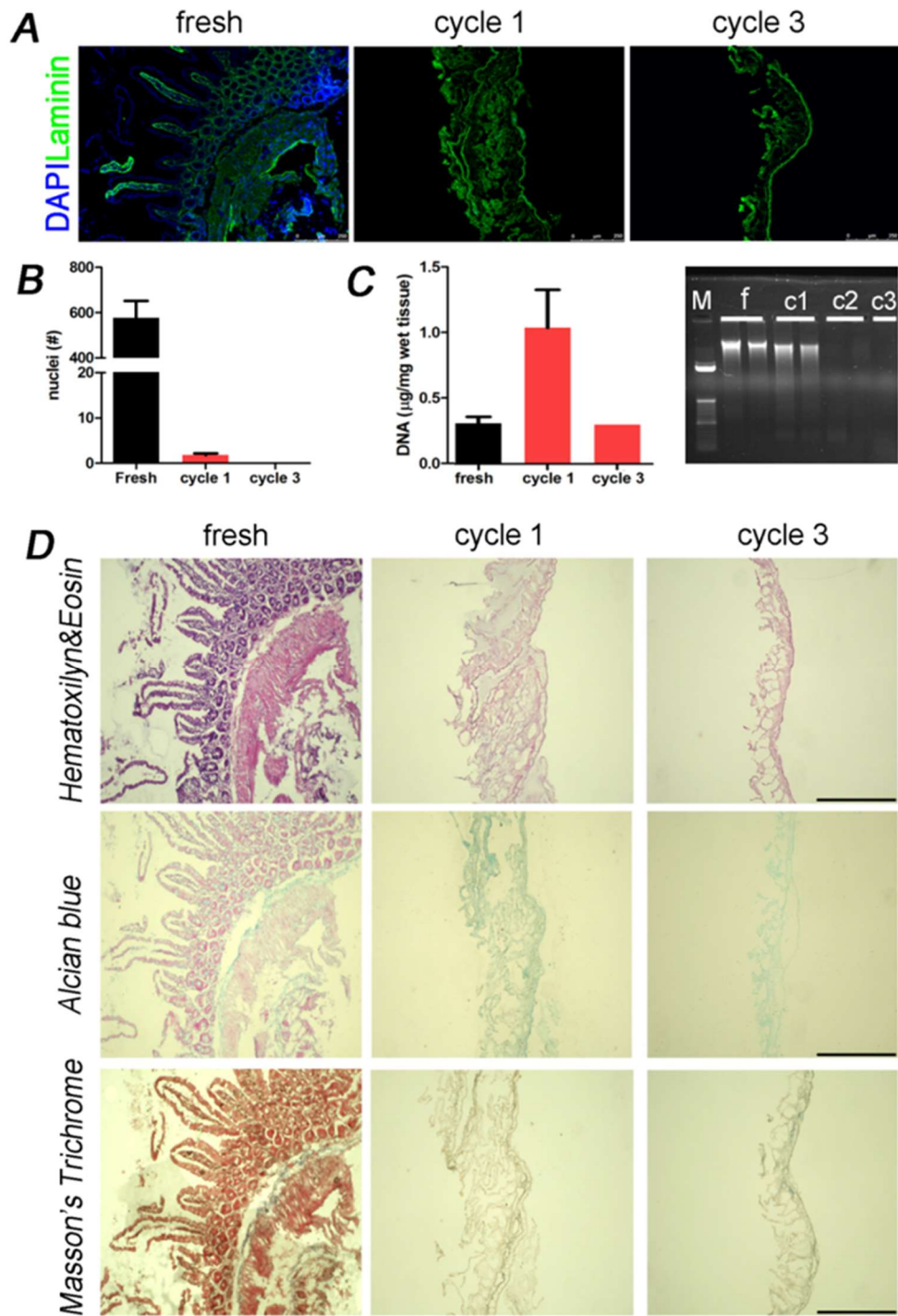


Fig. 6. Characterization of Intestine ECM after decellularization. Results after 3 DET cycles. Immunofluorescence (A), Nuclei quantification (B), DNA quantification (C), and ECM Components (D) are reported.

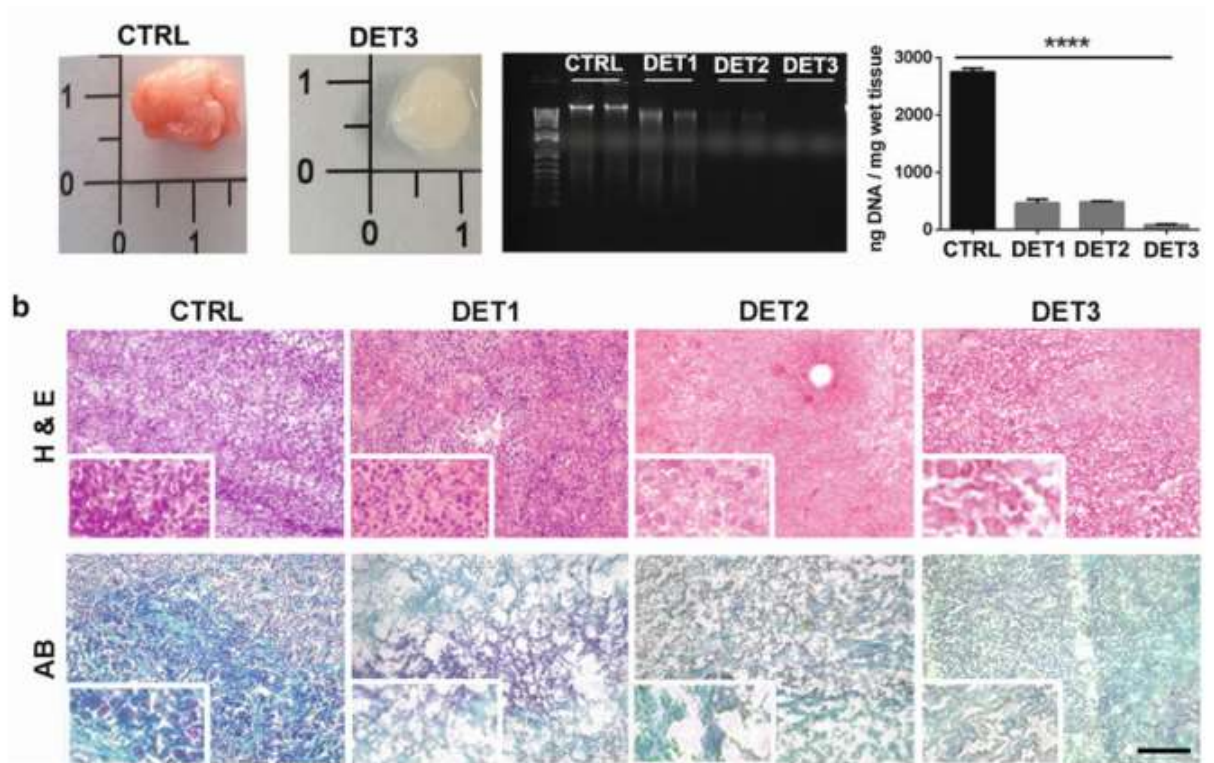


Fig. 7. Results of characterization of ARMS scaffold. Decellularization protocol and efficiency of the procedure. (a) Different phases of the protocol. Gross appearance of fresh and decellularized sample. DNA quantification and agarose gel. (b) Upper row: Hematox- ylin Eosin; lower row: Alcian blue (AB) at different cycles. Nuclei are depleted but tissue shape is maintained at different cycles. Scale bar: 50  $\mu$ m \*\*\*\* $p$ <0.0001. From Pozzobon et al. Alveolar Rhabdomyosarcoma Decellularization. *Methods Mol Biol.* 2017 May 25.

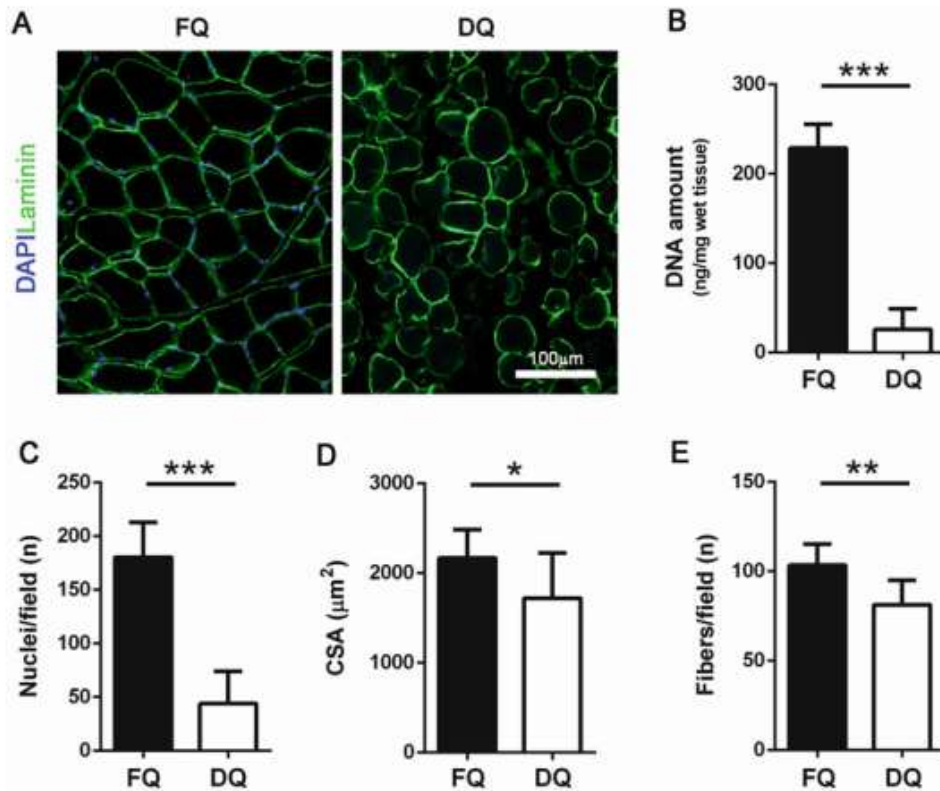


Fig. 8. Decellularization efficiency for quadricep scaffold. (a) Representative images of fresh and decellularized samples. (b) DNA amount quantification. (c) Quantification of the number of nuclei per field. (d) Evaluation of cross sectional area (CSA) of muscle fibers. (e) Quantification of the number of fibers per field. \*  $p < .05$ ; \*\*  $p < .01$ ; \*\*\*  $p < .001$ . From Piccoli et al. Mouse Skeletal Muscle Decellularization. *Methods Mol Biol.* 2017 Apr 28.

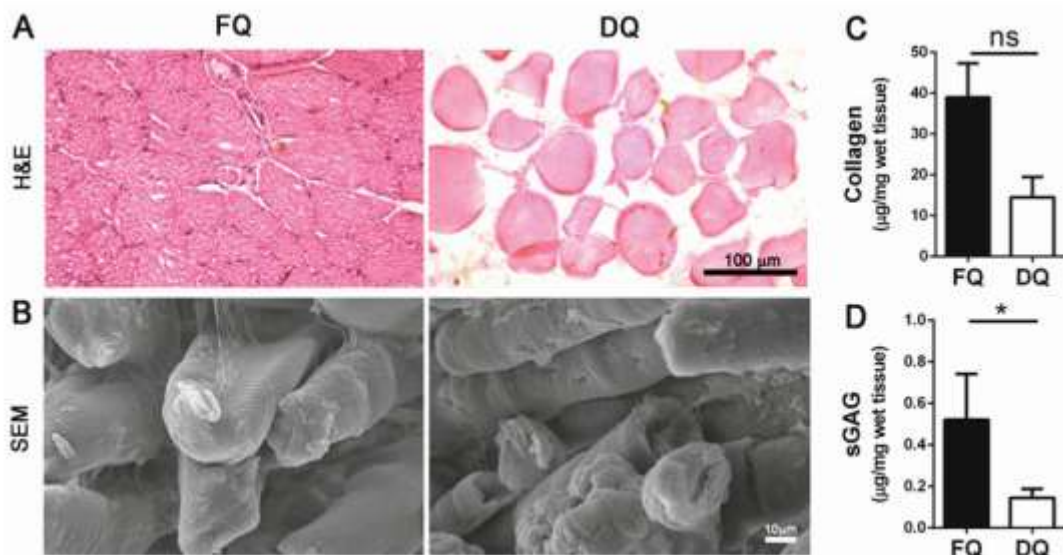


Fig. 9. Extracellular quadricep matrix (ECM) preservation. (a) Representative images of Hematoxylin & Eosin (H&E) stain on fresh and decellularized samples. (b) Scanning electron microscopy (SEM) images of fresh and decellularized quadriceps. (c) Quantification of collagen on muscle samples. (d) Quantification of sulphated glycosaminoglycan (sGAG) of fresh and decellularized muscles. \*  $p < .05$ . From Piccoli et al. Mouse Skeletal Muscle Decellularization. *Methods Mol Biol.* 2017 Apr 28.



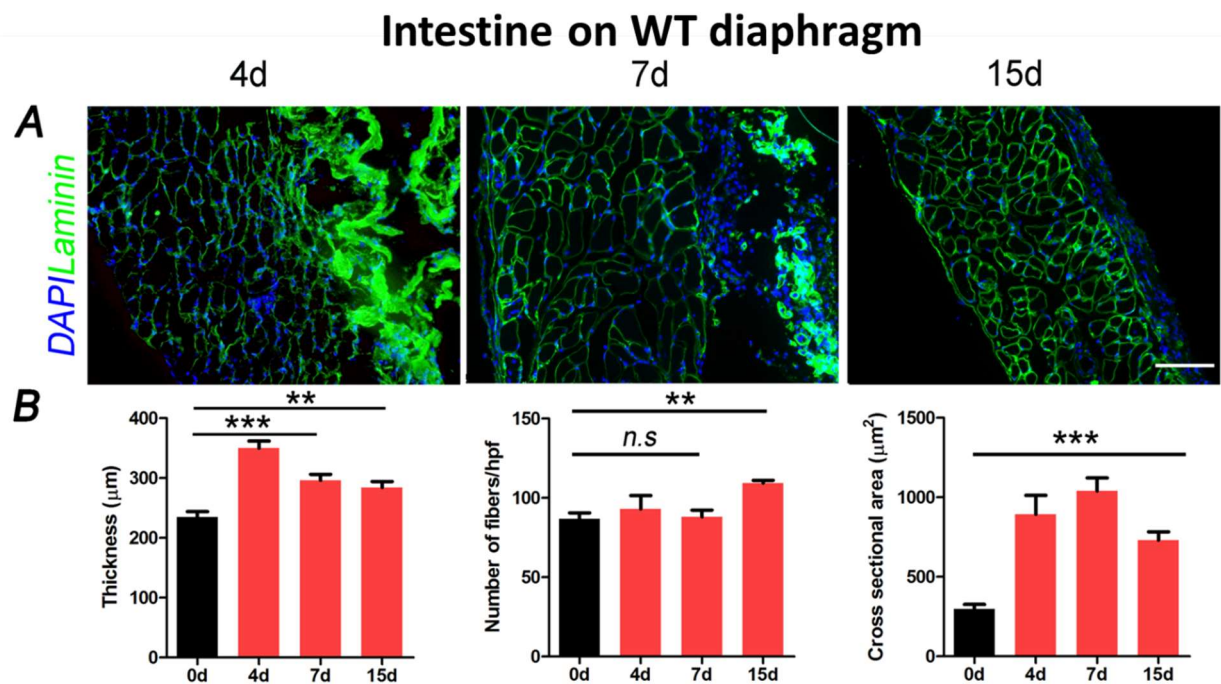


Fig. 11. Immunofluorescence (A) and histologic measurements (B) after implantation of intestine scaffolds on diaphragm.

### Volume muscle loss model.

#### *Histological analysis*

Figure 12 and 13 shows histologic findings at 7 and 15 days after scaffolds implantation on tibialis anterior. Staining for H&E and Masson's Trichromic (MT) are reported as morphologic results.

At 7 days quadriceps scaffold stimulates a reparative reorganization of muscular fibers. Indeed, confines of the damage are characterized by regularly oriented cells towards a reparative process. MT staining shows a difference in collagen quantity between the native muscle and the scaffold, but a migration of muscle cells inside the latter is already detectable. Skin, intestine and ARMS scaffold applied on muscle did not show muscle fibers regeneration at the edge of the damage neither an architectural pattern similar to muscle. ARMS scaffold is the most similar to the quadriceps one but no regeneration is

induced after its implantation. MT staining unveils a sharp separation between the skin scaffold and the muscle as a result of lack in integration. Moreover, MT staining underlines that no muscle cells are shown to be present inside the scaffold derived from skin, intestine and ARMS.

At 15 days after implantation of quadricep scaffold, regeneration and repair of muscle improved. A regularly organized structure and real myofibers are visible in the area of the scaffold and along the damage line. Histology of quadricep implants showed also the presence of new blood vessels inside the scaffold supporting the regenerative process. On contrary, skin and intestine implantation resulted in a completely disarranged structure of the muscle suggesting that no reparative nor regenerative processes are present. On MT staining it is also evident how these scaffolds are progressively reabsorbed. ARMS scaffold implantation at 15 days shows a diffuse infiltration of lymphocytes and monocytes suggesting an immunological response by the host. Even if this kind of response is fundamental in reparative process, no signs of regenerated muscle is visible 15 days after implantation of ARMS.

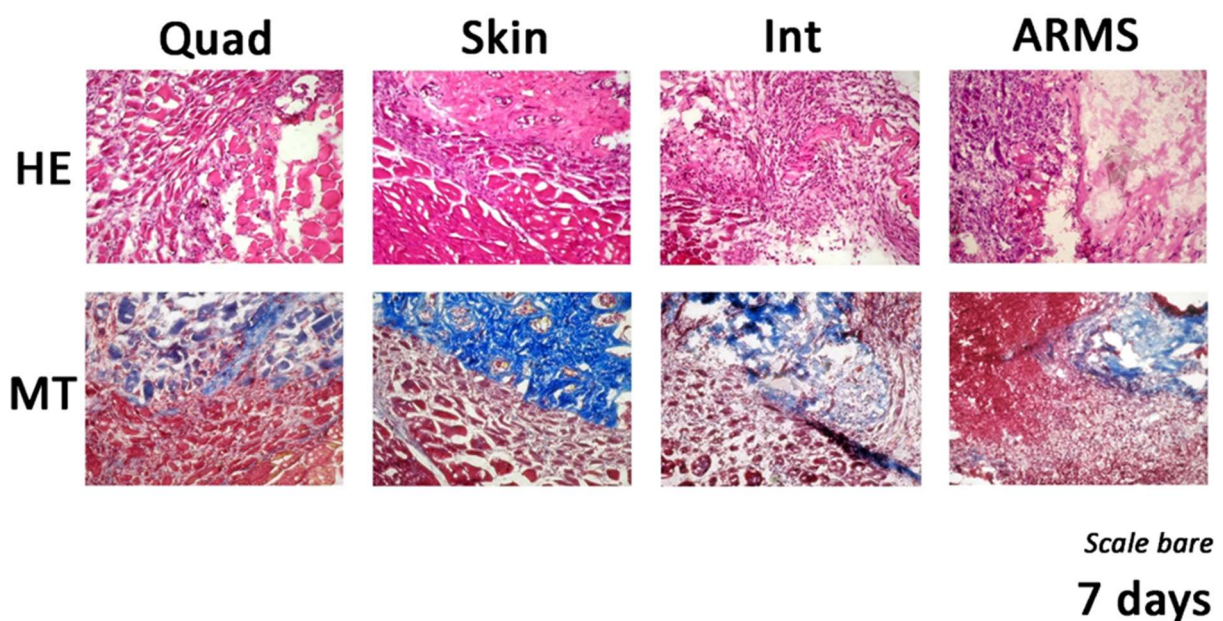


Fig. 12. Histological findings at 7 days after implantation in a VML model.

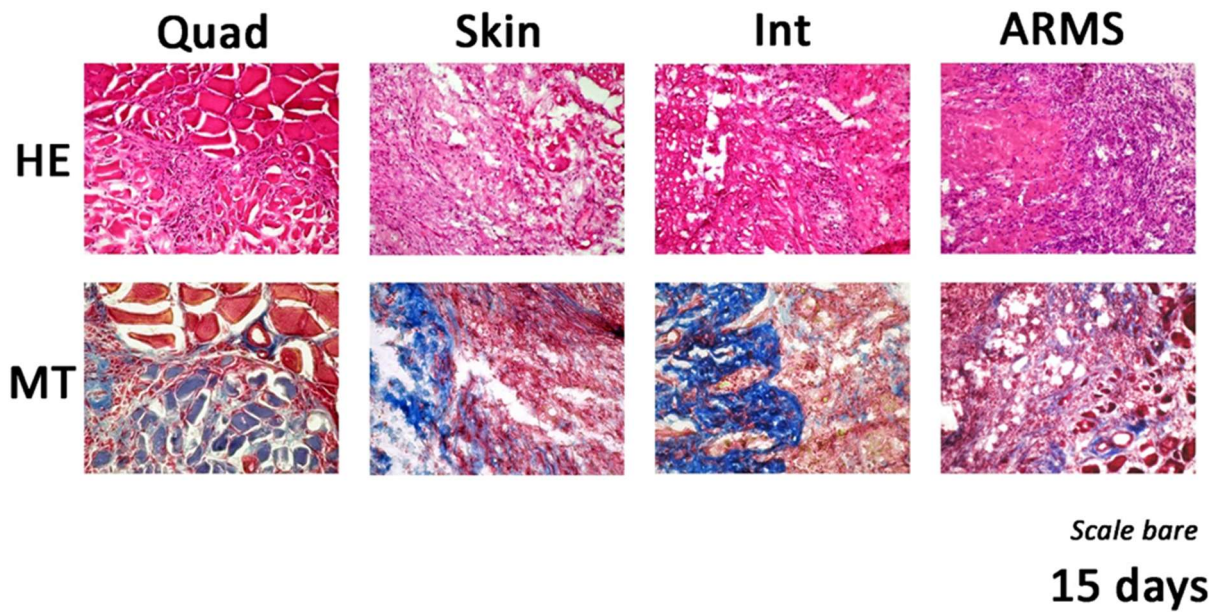


Fig. 13. Histological findings at 15 days after implantation in a VML model.

### ***Immunofluorescence and qRT-PCR***

Figures 14 and 15 shows results of immunofluorescence in VML model.

Immunofluorescence stainings were focused on macrophagic response (CD68) and new myofibers formation (Myogenin). As seen above, macrophages are fundamental in reparative and regenerative processes. Stainings for DAPI and laminin are also present to detect nuclei and muscular cells.

At 7 days after implantation macrophages surround the quadricep scaffold where new small centre-nucleated myofibers are also visible (Laminin+, DAPI+, Myogenin+). Skin and intestine scaffold are surrounded by macrophages demonstrating the activity of immune response but no regenerated myofibers are detectable. ARMS evokes a macrophagic response and small myofibers are visible but no central nuclei are visible suggesting an anomalous cellular regeneration.

Myogenin staining is specific for newly regenerated myofibers and it is detectable only in quadricep samples.

At 7 days post ECM implant Myogenin is detectable only in quadriceps treated mice, demonstrating the complete maturation of myofibers. In this group, an organized structure and disposition of myofibers is visible. At the later time point, 15 days, in all treated group Myogenin is absent.

In ARMS repaired muscle, scattered small myofibers are visible but they are not organized into a normal muscular architecture. In skin and intestine repaired muscle no regenerated myofibers are present in the damage area. CD68 staining shows that macrophages are still active at 15 days after implantation but with different patterns. In quadricep treated mice macrophages distribution is uniform around the contact area between the scaffold and the native muscle, while in the other treated mice their presence is weaker and more scattered.

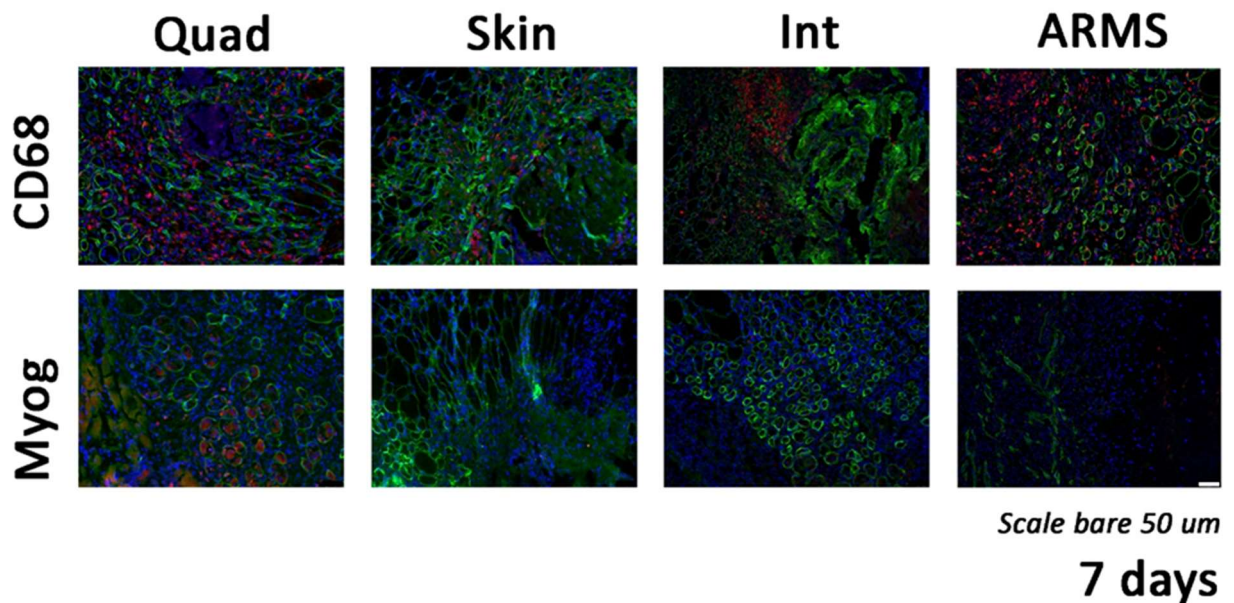


Fig. 14. Immunofluorescence study at 7 days after implantation in VML model. DAPI (blue), Laminin (green), CD68 and Myogenin (red in corresponding rows).

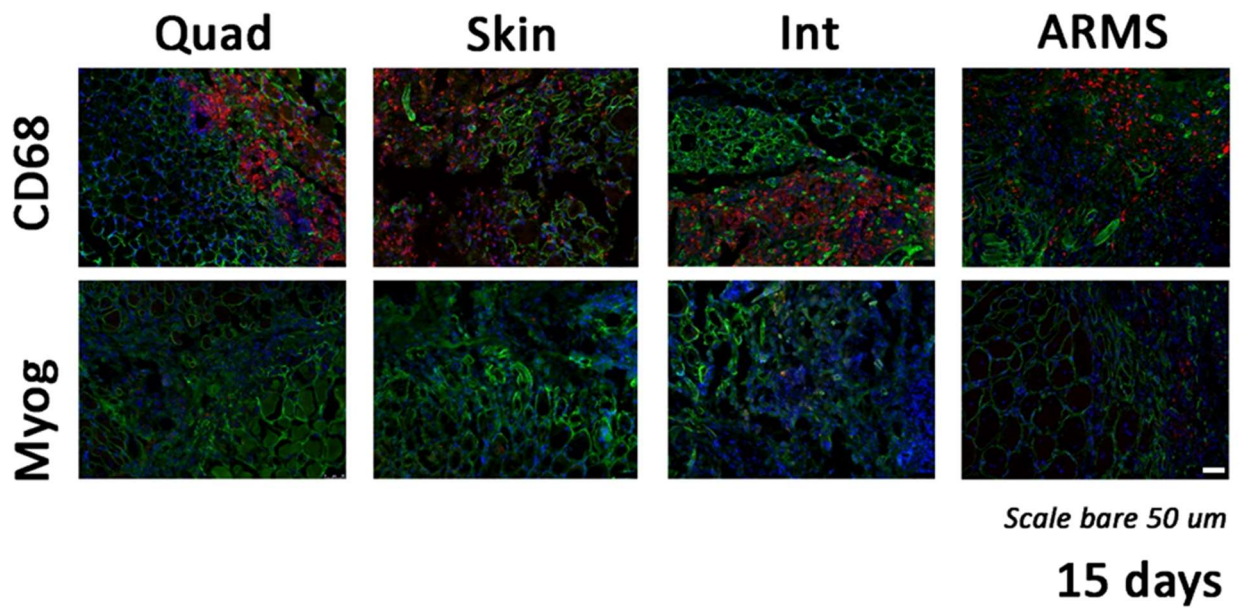


Fig. 15. Immunofluorescence study at 15 days after implantation in VML model. DAPI (blue), Laminin (green), CD68 and Myogenin (red in corresponding rows).

In parallel to the staining against the pan macrophages CD68, we performed gene expression for the macrophages polarized toward M1 (iNOS2) – involved in inflammation - and M2 (Arginase I) – involved in regeneration process. As shown in figure 16, at 7 and 15 days the damage alters the homeostasis of the muscle, but we did not detect significant pro regenerative response with none of the implanted ECM. It will be important to consider earlier and later time points to evaluate better the role of both M1 and M2 as inflammatory and regenerative macrophages respectively. We also analysed the gene expression of the embryonic myosin heavy chain (MHC3) and Myogenin, usually present during the early phases of myofiber regeneration. It was evident how the damage stimulated these genes but none of the implanted ECM really enhanced them, for the analysed time points.

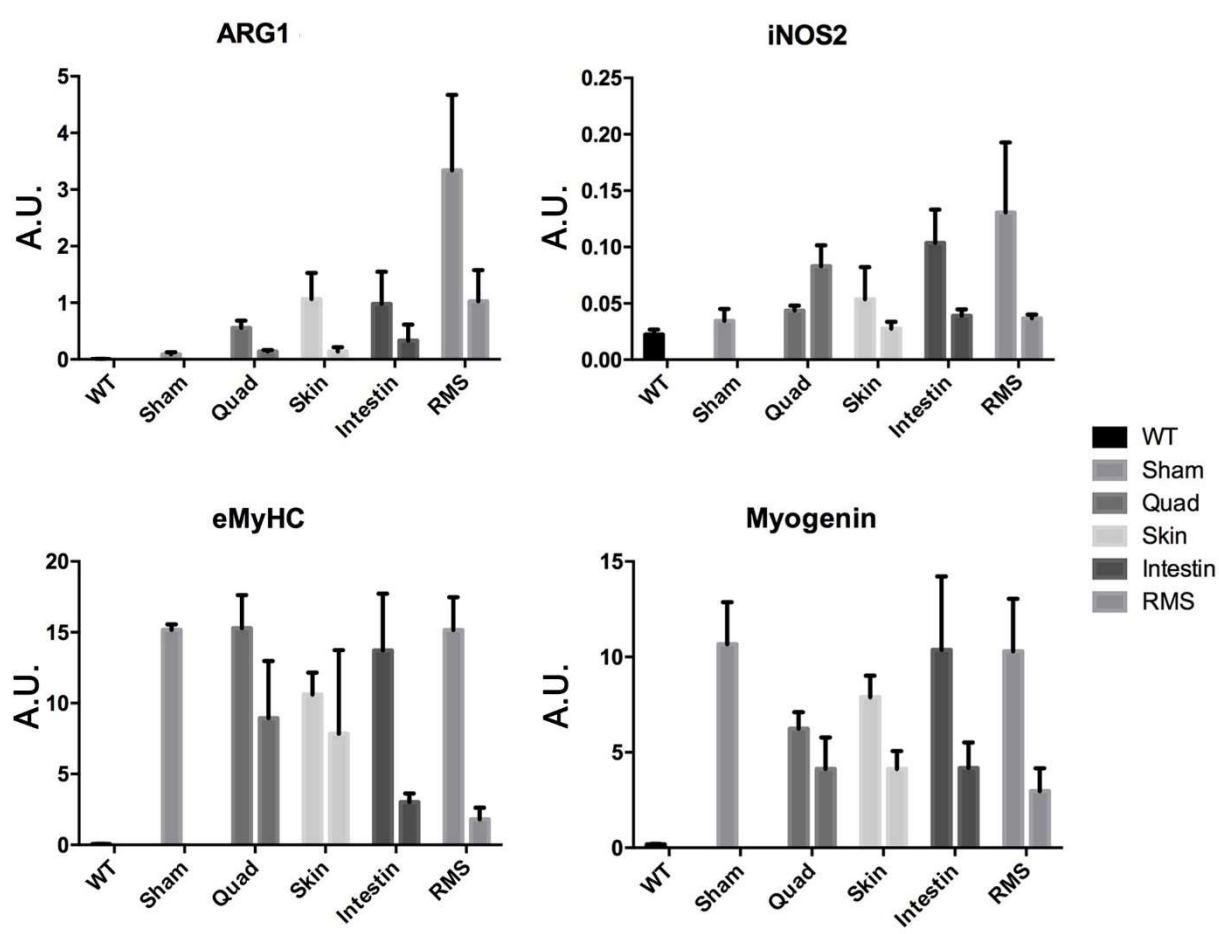


Fig. 16. Real time PCR. Data at 7 and 15 days post-implantation are shown for each scaffold.

# Discussion

The treatment of diseases related to muscular defects represents a challenge for clinicians. In this study models of congenital diaphragmatic hernia (CDH) and volume muscle loss (VML) have been proposed. These models stand for two different origin of muscular defect, the first due to congenital malformation and the second to traumatic or surgical ablation.

CDH is a rare and severe condition in which abdominal organs herniate in the thorax through a diaphragmatic defect in association to a significant lung hypoplasia. Treatment is based on intensive care resuscitation at birth and then surgical repair of the defect. Despite all the efforts to improve survival in CDH, mortality remains high [68]. When feasible, repair can be led through primary suture of the defect or by interposition of a prosthetic patch. Materials used for patches are usually artificial and connected to several complications and comorbidities, also with long-term onset. Infection, hernia recurrence, scoliosis, hernia recurrence, gastro-oesophageal reflux, and thorax deformities are the most cited complications related to use of synthetic patches [69].

VML typically results from traumatic incidents or surgical resections mainly due to tumors or infections. These injuries may lead to extensive loss of muscle and of its basement membrane significantly compromising functionality and quality of life of patients [70]. While skeletal muscle has innate capability to repair limited injuries, this does not happen with large-scale lesions. This is maybe related to the loss of muscle template and growth factor reservoir. Nowadays VML injuries are treated by transposition on skeletal muscle from a donor site of the same patient. This procedure has limited results in terms of functionality and it is affected by several complications such as infection and graft failure with necrosis [71].

In both cases of malformed or injured muscle, it is of primary relevance to obtain a bioscaffold suitable for muscle repairing and regeneration. Properties of the ideal bioscaffold are support to cell alignment, promotion of muscle formation in association with development of vascularization and innervation. Extracellular matrix (ECM) is nowadays investigated potentially as the ideal platform for a muscular scaffold. ECM, indeed, preserves the complex ultrastructure surrounding and supporting cells. Moreover, it retains angiogenic and growth factors that are fundamental in chemotactic process of tissutal regeneration.

This study is a continuation of a wider project aiming to investigate and produce a muscle ECM derived scaffold. Previous study from our group on diaphragmatic scaffold production and characterization has been published [65]. Using the same decellularization protocol of the present study, they obtained murine diaphragmatic ECM scaffold preserving most of the ultrastructural, physic-mechanical, and molecular properties of the fresh tissue. They applied the diaphragmatic scaffold on diaphragm of healthy and dystrophic mice demonstrating that a pro-regenerative environment and remodelling were elicited. Host diaphragm in contact with the scaffold, indeed, showed increase in thickness due to formation of real new generated myofibers and not to a foreign body reaction-like increase of cross sectional area. The environment, demonstrated to be stimulated towards regeneration as the observed switch between macrophagic M1 and M2 subtype was observed. No immunoresponse toward rejection was evident.

In the present study we wanted to explore the efficacy of the detergent-enzymatic protocol applied for different tissues. Moreover, using scaffolds derived from different tissues, we investigated the role of tissue specificity of the scaffold in relation to regenerative potential.

Detergent Enzymatic decellularization protocol was based on association of Sodium Deoxycholate (for skin, intestine and quadriceps), Sodium dodecyl sulphate (for

rhabdomyosarcoma) [80] and DNAase I [72]. Nuclear and DNA depletion is fundamental to avoid immune-related rejection of the scaffold as it leads to the removal of MHC-I and MHC-II antigens [74]. At the same time residual extracellular matrix maintains same ultrastructural and composition characteristics. Ultrastructural and chemotactic properties retained in the ECM are fundamental in driving cell migration, differentiation and maturation in a pro-regenerative process. With skin, intestine and ARMS we observed decellularization results comparable to that obtained in diaphragmatic tissue. Residing on these observations we can speculate that the abnormal muscle regeneration elicited by those scaffold is not related to alteration of ECM but to the intrinsic characteristics of the matrix itself.

In vivo application of skin and intestine on diaphragm resulted in anomalous remodelling of native muscle. Even if a migration of cells inside the scaffold was observed, no regeneration of muscle was evident. Indeed, increase in thickness of native diaphragm corresponded to a parallel increase in cross sectional area of myofibers. This reaction could be related to an inflammatory response towards a foreign body leading to hypertrophy of the native tissue surrounding the scaffold. This was not observed by Piccoli et al with diaphragmatic scaffold implantation as signs of newly regenerated myofibers were evident: increasing thickness corresponded to a more significant increase in number of centre nucleated myofibers without cross sectional area augmentation. Also scaffold derived from intestine and skin showed a progressive reabsorbance confirming the degradation fate that classically distinguishes biological scaffolds [73].

In order to investigate a model of volume muscle loss injury, experiments on tibialis anterioris muscle was conducted. In this part of the experiment we wanted to compare skeletal muscle scaffold to other derived from different tissues. Implantation of quadriceps scaffold elicited damage repair through regeneration of new myofibers. In the contact area between scaffold and muscle, indeed, new centre-nucleated myofibers are visible

arranging into parallel disposition typical of muscular tissue. Moreover, examining myogenin staining, marker expressed during the first stages of myogenesis that is switched off when myofibers are completely formed, we demonstrated that only in quadriceps visible myofibers are really newly regenerated. The implantation of scaffold derived from skin and intestine did not show any stimulus toward regeneration. New myofibers or muscle-like cells were not observed in the area of the scaffold while a rearrangement of native muscle was evoked as a sign of reparation and reaction for tissue remodelling. Differences in regenerative efficacy may reside in the origin of the scaffold and this is a further demonstration that different 3D architecture and composition of the ECM give not the correct signalling and stimulus towards correct regeneration. Indeed, ECM is capable to stimulate recruitment and proliferation of appropriate cell types involved in the regeneration process [75].

In this study we wanted also to test ECM derived from pathologic muscle. The aim was to investigate not only the effect of the biochemical factors present in pathological ECM but also the action of a disorganized pathological ECM muscle derived. We decided to use ECM derived from rhabdomyosarcoma (ARMS). Implantation of ARMS elicited the formation of myofibers inside the scaffold area but they arranged into a not organized muscular pattern. Moreover, such generated myofibers appeared scattered, small and not centre-nucleated giving the suspicion that they may not be adequate for a real muscle regeneration. These observations on ARMS scaffold indicate that illness alters also composition and properties of tissue even if the origin is the same.

Gene expression for embryonic myosin heavy chain and myogenin after 7 and 15 days did not show a specific enhancement, further analysis of both gene for early and later time point are planned.

Angiogenic properties are fundamental in tissue engineering of muscle. Blood perfusion allows a tissue to be maintained and delivers cells and factors necessary to complete

regeneration. ECM usually possess angiogenic properties attracting endothelial cells to repopulate vessels structures in the matrix [76]. Consistently with other studies [74], in our study blood vessels were observed inside the muscle scaffold near the interface with damaged muscle. Interesting was that with implantation of different scaffold no signs of revascularization were visible. This difference may be of primary importance to delineate the basis for a bioscaffold-based regeneration. Generally, ECM retains angiogenic soluble factors (such as VEGF) [23] but mismatch in the structure of the tissue may affect also the revascularization process.

In VML part of the study a focus on macrophagic response has also been provided. It is known that macrophages can have different phenotypes modulated by soluble factors [77, 78] and that can influence the environment towards regeneration (M2 type) or perpetual inflammation (M1 type) [79]. In our experiment, macrophagic presence could be observed after implantation of all the scaffolds and also gene expression for M1 and M2 highlighted this homogeneous behaviour. Only after implantation of quadriceps ECM, new regenerated fibers were observed and we could postulate that also macrophages play a regenerative role. The other scaffolds did not show the same newly born fibers and this may reside in the anomalous implanted ECM structure that did not drove adequate regenerative signalling from the microenvironment and from the macrophages.

Results obtained with rtPCR analysis did not provide significant results in terms of regeneration of new myofibers and antiflogistic (proregenerative) environment. We consider that investigations on earlier and later time points may reveal a deeper characterization on these aspects.

## Conclusions

This study is a part of a wider project aiming to create a valid substitute for skeletal muscle based on bioscaffold derived from extracellular matrix. This kind of bioscaffold seems to be the most reliable in terms of immunoresponse and pro-regenerative properties.

In this study the tissue-specificity resulted as a fundamental aspect to obtain the best response from the scaffold. A tissue specific bioscaffold for muscle carries all the structural, chemotactic, pro-angiogenic, and immune-modulating requisites in order to obtain a real regeneration of a functional skeletal muscle. The involvement of ECM-based scaffold derived from different tissue may lead to a perpetual foreign body-like response compromising the deposition of muscular tissue.

Investigations on rhabdomyosarcoma allowed to confirm that in diseased tissue and organs extracellular matrix is affected with significative alteration of its properties.

Many investigations on muscle ECM-derived bioscaffold are still needed before a clinical trial can be set. Deep investigations on angiogenic properties of the scaffold are undergoing to reveal another fundamental side of regenerative potential of extracellular matrix.

## Bibliography

- 1) Chargé SB, Rudnicki MA. Cellular and molecular regulation of muscle regeneration. *Physiol Rev.* 2004 Jan;84(1):209-38.
- 2) Rudnicki MA, Schnegelsberg PN, Stead RH, Braun T, Arnold HH, Jaenisch R. MyoD or Myf-5 is required for the formation of skeletal muscle. *Cell.* 1993 Dec 31;75(7):1351-9.
- 3) Tidball JG. Inflammatory processes in muscle injury and repair. *Am J Physiol Regul Integr Comp Physiol.* 2005 Feb;288(2):R345-53.
- 4) Teixeira CF1, Zamunér SR, Zuliani JP, Fernandes CM, Cruz-Hofling MA, Fernandes I, Chaves F, Gutiérrez JM. Neutrophils do not contribute to local tissue damage, but play a key role in skeletal muscle regeneration, in mice injected with Bothrops asper snake venom. *Muscle Nerve* 2003 Oct;28(4):449-59.
- 5) Arnold L, Henry A, Poron F, Baba-Amer Y, van Rooijen N, Plonquet A, Gherardi RK, Chazaud B. Inflammatory monocytes recruited after skeletal muscle injury switch into antiinflammatory macrophages to support myogenesis. *J Exp Med.* 2007 May 14;204(5):1057-69.
- 6) Saclier M, Cuvellier S, Magnan M, Mounier R, Chazaud B. Monocyte/macrophage interactions with myogenic precursor cells during skeletal muscle regeneration. *FEBS J.* 2013 Sep;280(17):4118-30.
- 7) Chazaud B, Brigitte M, Yacoub-Youssef H, Arnold L, Gherardi R, Sonnet C, Lafuste P, Chretien F. Dual and beneficial roles of macrophages during skeletal muscle regeneration. *Exerc Sport Sci Rev.* 2009 Jan;37(1):18-22.
- 8) Mauro A. Satellite cell of skeletal muscle fibers. *J Biophys Biochem Cytol.* 1961 Feb;9:493-5.

- 9) Scharner J, Zammit PS. The muscle satellite cell at 50: the formative years. *Skelet Muscle* 2011 Aug 17;1(1):28.
- 10) Zammit PS, Golding JP, Nagata Y, Hudon V, Partridge TA, Beauchamp JR. Muscle satellite cells adopt divergent fates: a mechanism for self-renewal? *J Cell Biol.* 2004 Aug 2;166(3):347-57.
- 11) Fukada S, Uezumi A, Ikemoto M, Masuda S, Segawa M, Tanimura N, Yamamoto H, Miyagoe-Suzuki Y, Takeda S. Molecular signature of quiescent satellite cells in adult skeletal muscle. *Stem Cells.* 2007 Oct;25(10):2448-59.
- 12) Yablonka-Reuveni Z, Rudnicki MA, Rivera AJ, Primig M, Anderson JE, Natanson P. The transition from proliferation to differentiation is delayed in satellite cells from mice lacking MyoD. *Dev Biol.* 1999 Jun 15;210(2):440-55.
- 13) Relaix F, Zammit PS. Satellite cells are essential for skeletal muscle regeneration: the cell on the edge returns centre stage. *Development.* 2012 Aug;139(16):2845-56.
- 14) De Angelis L, Berghella L, Coletta M, Lattanzi L, Zanchi M, Cusella-De Angelis MG, Ponzetto C, Cossu G. Skeletal myogenic progenitors originating from embryonic dorsal aorta coexpress endothelial and myogenic markers and contribute to postnatal muscle growth and regeneration. *J Cell Biol.* 1999 Nov 15;147(4):869-78.
- 15) Tamaki T, Akatsuka A, Ando K, Nakamura Y, Matsuzawa H, Hotta T, Roy RR, Edgerton VR. Identification of myogenic-endothelial progenitor cells in the interstitial spaces of skeletal muscle. *J Cell Biol.* 2002 May 13;157(4):571-7.
- 16) Mitchell KJ, Pannérec A, Cadot B, Parlakian A, Besson V, Gomes ER, Marazzi G, Sassoon DA. Identification and characterization of a non-satellite

- cell muscle resident progenitor during postnatal development. *Nat Cell Biol.* 2010 Mar;12(3):257-66.
- 17) Asakura A, Seale P, Girgis-Gabardo A, Rudnicki MA. Myogenic specification of side population cells in skeletal muscle. *J Cell Biol.* 2002 Oct 14;159(1):123-34.
- 18) Uezumi A, Fukada S, Yamamoto N, Takeda S, Tsuchida K. Mesenchymal progenitors distinct from satellite cells contribute to ectopic fat cell formation in skeletal muscle. *Nat Cell Biol.* 2010 Feb;12(2):143-52.
- 19) Joe AW, Yi L, Natarajan A, Le Grand F, So L, Wang J, Rudnicki MA, Rossi FM. Muscle injury activates resident fibro/adipogenic progenitors that facilitate myogenesis. *Nat Cell Biol.* 2010 Feb;12(2):153-63.
- 20) Mutsaers SE, Bishop JE, McGrouther G, Laurent GJ. Mechanisms of tissue repair: from wound healing to fibrosis. *Int J Biochem Cell Biol.* 1997 Jan;29(1):5-17.
- 21) Mozdziak PE, Pulvermacher PM, Schultz E. Muscle regeneration during hindlimb unloading results in a reduction in muscle size after reloading. *J Appl Physiol (1985).* 2001 Jul;91(1):183-90
- 22) Mitchell PO, Pavlath GK. Skeletal muscle atrophy leads to loss and dysfunction of muscle precursor cells. *Am J Physiol Cell Physiol.* 2004 Dec;287(6):C1753-62.
- 23) Badylak SF. Xenogeneic extracellular matrix as a scaffold for tissue reconstruction. *Transpl Immunol.* 2004 Apr;12(3-4):367-77.
- 24) Badylak SF, Freytes DO, Gilbert TW. Reprint of: Extracellular matrix as a biological scaffold material: Structure and function. *Acta Biomater.* 2015 Sep;23 Suppl:S17-26.

- 25) Teodori L, Costa A, Marzio R, Perniconi B, Coletti D, Adamo S, Gupta B, Tarnok A. Native extracellular matrix: a new scaffolding platform for repair of damaged muscle. *Front Physiol.* 2014 Jun 16;5:218.
- 26) Wolf MT, Daly KA, Reing JE, Badylak SF. Biologic scaffold composed of skeletal muscle extracellular matrix. *Biomaterials.* 2012 Apr;33(10):2916-25.
- 27) Daley WP, Peters SB, Larsen M. Extracellular matrix dynamics in development and regenerative medicine. *J Cell Sci.* 2008 Feb 1;121(Pt 3):255-64.
- 28) Gilbert PM, Havenstrite KL, Magnusson KE, Sacco A, Leonardi NA, Kraft P, Nguyen NK, Thrun S, Lutolf MP, Blau HM. Substrate elasticity regulates skeletal muscle stem cell self-renewal in culture. *Science* 2010 Aug 27;329(5995):1078-81.
- 29) Stern MM, Myers RL, Hammam N, Stern KA, Eberli D, Kritchevsky SB, Soker S, Van Dyke M. The influence of extracellular matrix derived from skeletal muscle tissue on the proliferation and differentiation of myogenic progenitor cells ex vivo. *Biomaterials.* 2009 Apr;30(12):2393-9.
- 30) Badylak SF, Lantz GC, Coffey A, Geddes LA. Small intestinal submucosa as a large diameter vascular graft in the dog. *J Surg Res.* 1989 Jul;47(1):74-80.
- 31) Piechota HJ, Dahms SE, Probst M, Gleason CA, Nunes LS, Dahiya R, Lue TF, Tanagho EA. Functional rat bladder regeneration through xenotransplantation of the bladder acellular matrix graft. *Br J Urol.* 1998 Apr;81(4):548-59.
- 32) Perniconi B, Costa A, Aulino P, Teodori L, Adamo S, Coletti D. The pro-myogenic environment provided by whole organ scale acellular scaffolds from skeletal muscle. *Biomaterials.* 2011 Nov;32(31):7870-82.

- 33) Olson JL, Atala A, Yoo JJ. Tissue engineering: current strategies and future directions. *Chonnam Med J* 2011 Apr;47(1):1-13.
- 34) Lü SH, Wang HB, Liu H, Wang HP, Lin QX, Li DX, Song YX, Duan CM, Feng LX, Wang CY. Reconstruction of engineered uterine tissues containing smooth muscle layer in collagen/matrigel scaffold in vitro. *Tissue Eng Part A*. 2009 Jul;15(7):1611-8.
- 35) Okano T, Matsuda T. Hybrid muscular tissues: preparation of skeletal muscle cell-incorporated collagen gels. *Cell Transplant*. 1997 Mar-Apr;6(2):109-18.
- 36) Okano T, Matsuda T. Tissue engineered skeletal muscle: preparation of highly dense, highly oriented hybrid muscular tissues. *Cell Transplant* 1998 Jan-Feb;7(1):71-82.
- 37) Chiron S, Tomczak C, Duperray A, Lainé J, Bonne G, Eder A, Hansen A, Eschenhagen T, Verdier C, Coirault C. Complex interactions between human myoblasts and the surrounding 3D fibrin-based matrix. *PLoS One*. 2012;7(4):e36173.
- 38) Badylak SF, Weiss DJ, Caplan A, Macchiarini P. Engineered whole organs and complex tissues. *Lancet*. 2012 Mar 10;379(9819):943-52.
- 39) Derwin KA, Baker AR, Spragg RK, Leigh DR, Iannotti JP. Commercial extracellular matrix scaffolds for rotator cuff tendon repair. Biomechanical, biochemical, and cellular properties. *J Bone Joint Surg Am*. 2006 Dec;88(12):2665-72.
- 40) Freytes DO, Stoner RM, Badylak SF. Uniaxial and biaxial properties of terminally sterilized porcine urinary bladder matrix scaffolds. *J Biomed Mater Res B Appl Biomater*. 2008 Feb;84(2):408-14.

- 41) Prevel CD, Eppley BL, Summerlin DJ, Sidner R, Jackson JR, McCarty M, Badylak SF. Small intestinal submucosa: utilization as a wound dressing in full-thickness rodent wounds. *Ann Plast Surg.* 1995 Oct;35(4):381-8.
- 42) Cobb MA, Badylak SF, Janas W, Boop FA. Histology after dural grafting with small intestinal submucosa. *Surg Neurol.* 1996 Oct;46(4):389-93.
- 43) Dejardin LM, Arnoczky SP, Clarke RB. Use of small intestinal submucosal implants for regeneration of large fascial defects: an experimental study in dogs. *J Biomed Mater Res.* 1999 Aug;46(2):203-11.
- 44) Kropp BP. Developmental aspects of the contractile smooth muscle component in small intestinal submucosa regenerated urinary bladder. *Adv Exp Med Biol.* 1999;462:129-35.
- 45) Shalhav AL, Elbahnasy AM, Bercowsky E, Kovacs G, Brewer A, Maxwell KL, McDougall EM, Clayman RV. Laparoscopic replacement of urinary tract segments using biodegradable materials in a large-animal model. *J Endourol.* 1999 May;13(4):241-4.
- 46) Portis AJ, Elbahnasy AM, Shalhav AL, Brewer A, Humphrey P, McDougall EM, Clayman RV. Laparoscopic augmentation cystoplasty with different biodegradable grafts in an animal model. *J Urol.* 2000 Oct;164(4):1405-11.
- 47) Lecheminant J1, Field C. Porcine urinary bladder matrix: a retrospective study and establishment of protocol. *J Wound Care.* 2012 Oct;21(10):476, 478-80, 482.
- 48) Kruper GJ, Vandegriend ZP, Lin HS, Zuliani GF. Salvage of failed local and regional flaps with porcine urinary bladder extracellular matrix aided tissue regeneration. *Case Rep Otolaryngol.* 2013;2013:917183.

- 49) Brennan EP, Reing J, Chew D, Myers-Irvin JM, Young EJ, Badylak SF. Antibacterial activity within degradation products of biological scaffolds composed of extracellular matrix. *Tissue Eng.* 2006 Oct;12(10):2949-55.
- 50) Turner NJ, Badylak JS, Weber DJ, Badylak SF. Biologic scaffold remodeling in a dog model of complex musculoskeletal injury. *J Surg Res.* 2012 Aug;176(2):490-502.
- 51) Perniconi B, Costa A, Aulino P, Teodori L, Adamo S, Coletti D. The pro-myogenic environment provided by whole organ scale acellular scaffolds from skeletal muscle. *Biomaterials* 2011 Nov;32(31):7870-82.
- 52) AR1, Smith LR, Lieber RL, Varghese S. Method for decellularizing skeletal muscle without detergents or proteolytic enzymes. *Tissue Eng Part C Methods.* 2011 Apr;17(4):383-9.
- 53) Badylak SF, Taylor D, Uygun K. Whole-organ tissue engineering: decellularization and recellularization of three-dimensional matrix scaffolds. *Annu Rev Biomed Eng.* 2011 Aug 15;13:27-53.
- 54) Crapo PM, Gilbert TW, Badylak SF. An overview of tissue and whole organ decellularization processes. *Biomaterials.* 2011 Apr;32(12):3233-43.
- 55) Ott HC, Matthiesen TS, Goh SK, Black LD, Kren SM, Netoff TI, Taylor DA. Perfusion-decellularized matrix: using nature's platform to engineer a bioartificial heart. *Nat Med.* 2008 Feb;14(2):213-21.
- 56) Price AP, England KA, Matson AM, Blazar BR, Panoskaltsis-Mortari A. Development of a decellularized lung bioreactor system for bioengineering the lung: the matrix reloaded. *Tissue Eng Part A.* 2010 Aug;16(8):2581-91.
- 57) Shupe T, Williams M, Brown A, Willenberg B, Petersen BE. Method for the decellularization of intact rat liver. *Organogenesis* 2010 Apr-Jun;6(2):134-6.

- 58) Meyer SR, Chiu B, Churchill TA, Zhu L, Lakey JR, Ross DB. Comparison of aortic valve allograft decellularization techniques in the rat. *J Biomed Mater Res A*. 2006 Nov;79(2):254-62.
- 59) Lehr EJ, Rayat GR, Chiu B, Churchill T, McGann LE, Coe JY, Ross DB. Decellularization reduces immunogenicity of sheep pulmonary artery vascular patches. *J Thorac Cardiovasc Surg*. 2011 Apr;141(4):1056-62.
- 60) Deeken CR1, White AK, Bachman SL, Ramshaw BJ, Cleveland DS, Loy TS, Grant SA. Method of preparing a decellularized porcine tendon using tributyl phosphate. *J Biomed Mater Res B Appl Biomater*. 2011 Feb;96(2):199-206.
- 61) Baiguera S, Jungebluth P, Burns A, Mavilia C, Haag J, De Coppi P, Macchiarini P. Tissue engineered human tracheas for in vivo implantation. *Biomaterials*. 2010 Dec;31(34):8931-8.
- 62) Ozeki M, Narita Y, Kagami H, Ohmiya N, Itoh A, Hirooka Y, Niwa Y, Ueda M, Goto H. Evaluation of decellularized esophagus as a scaffold for cultured esophageal epithelial cells. *J Biomed Mater Res A*. 2006 Dec 15;79(4):771-8.
- 63) Reing JE, Brown BN, Daly KA, Freund JM, Gilbert TW, Hsiong SX, Huber A, Kullas KE, Tottey S, Wolf MT, Badylak SF. The effects of processing methods upon mechanical and biologic properties of porcine dermal extracellular matrix scaffolds. *Biomaterials*. 2010 Nov;31(33):8626-33.
- 64) Totonelli G, Maghsoudlou P, Garriboli M, Riegler J, Orlando G, Burns AJ, Sebire NJ, Smith VV, Fishman JM, Ghionzoli M, Turmaine M, Birchall MA, Atala A, Soker S, Lythgoe MF, Seifalian A, Pierro A, Eaton S, De Coppi PA. Rat decellularized small bowel scaffold that preserves villus-crypt architecture for intestinal regeneration. *Biomaterials*. 2012 Apr;33(12):3401-10.
- 65) Piccoli M, Urbani L, Alvarez-Fallas ME, Franzin C, Dedja A, Bertin E, Zuccolotto G, Rosato A, Pavan P, Elvassore N, De Coppi P, Pozzobon M.

- Improvement of diaphragmatic performance through orthotopic application of decellularized extracellular matrix patch. *Biomaterials*. 2016 Jan;74:245-55.
- 66) Dziki, J.L., et al. Immunomodulation and Mobilization of Progenitor Cells by Extracellular Matrix Bioscaffolds for Volumetric Muscle Loss Treatment. *Tissue Eng Part A*, 2016. 22(19-20): p. 1129-1139.
- 67) Kasukonis, B., et al. Codelivery of Infusion Decellularized Skeletal Muscle with Minced Muscle Autografts Improved Recovery from Volumetric Muscle Loss Injury in a Rat Model. *Tissue Eng Part A*, 2016. 22(19-20): p. 1151-1163.
- 68) Leeuwen L, Fitzgerald DA. Congenital diaphragmatic hernia. *J Paediatr Child Health*. 2014 Sep;50(9):667-73.
- 69) Fauza DO. Tissue engineering in congenital diaphragmatic hernia. *Semin Pediatr Surg*. 2014 Jun;23(3):135-40.
- 70) Heemskerk J, Kitslaar P. Acute compartment syndrome of the lower leg: retrospective study on prevalence, technique, and outcome of fasciotomies. *World J Surg*. 2003 Jun;27(6):744-7.
- 71) Eckardt A1, Fokas K. Microsurgical reconstruction in the head and neck region: an 18-year experience with 500 consecutive cases. *J Craniomaxillofac Surg*. 2003 Aug;31(4):197-201.
- 72) Conconi MT, Bellini S, Teoli D, De Coppi P, Ribatti D, Nico B, Simonato E, Gamba PG, Nussdorfer GG, Morpurgo M, Parnigotto PP. In vitro and in vivo evaluation of acellular diaphragmatic matrices seeded with muscle precursors cells and coated with VEGF silica gels to repair muscle defect of the diaphragm. *J Biomed Mater Res A*. 2009 May;89(2):304-16.

- 73) Gilbert TW, Stewart-Akers AM, Badylak SF. A quantitative method for evaluating the degradation of biologic scaffold materials. *Biomaterials*. 2007 Jan;28(2):147-50.
- 74) Fishman JM, Lowdell MW, Urbani L, Ansari T, Burns AJ, Turmaine M, North J, Sibbons P, Seifalian AM, Wood KJ, Birchall MA, De Coppi P. Immunomodulatory effect of a decellularized skeletal muscle scaffold in a discordant xenotransplantation model. *Proc Natl Acad Sci U S A*. 2013 Aug 27;110(35):14360-5.
- 75) Reing JE, Zhang L, Myers-Irvin J, Cordero KE, Freytes DO, Heber-Katz E, Bedelbaeva K, McIntosh D, Dewilde A, Braunhut SJ, Badylak SF. Degradation products of extracellular matrix affect cell migration and proliferation. *Tissue Eng Part A*. 2009 Mar;15(3):605-14.
- 76) Valentin JE, Badylak JS, McCabe GP, Badylak SF. Extracellular matrix bioscaffolds for orthopaedic applications. A comparative histologic study. *J Bone Joint Surg Am*. 2006 Dec;88(12):2673-86.
- 77) Mills CD, Kincaid K, Alt JM, Heilman MJ, Hill AM. M-1/M-2 macrophages and the Th1/Th2 paradigm. *J Immunol*. 2000 Jun 15;164(12):6166-73.
- 78) Philip R, Epstein LB. Tumour necrosis factor as immunomodulator and mediator of monocyte cytotoxicity induced by itself, gamma-interferon and interleukin-1. *Nature*. 1986 Sep 4-10;323(6083):86-9.
- 79) Tidball JG, Dorshkind K, Wehling-Henricks M. Shared signaling systems in myeloid cell-mediated muscle regeneration. *Development*. 2014 Mar;141(6):1184-96.
- 80) Pozzobon M, Saggiaro M, D'Agostino S, Bisogno G, Muraca M, Gamba P. Alveolar Rhabdomyosarcoma Decellularization. *Methods Mol Biol*. 2017 May 25.

81) Piccoli M, Trevisan C, Maghin E, Franzin C, Pozzobon M. Mouse Skeletal Muscle Decellularization. *Methods Mol Biol.* 2017 Apr 28.